Direct Back EMF Detection Method for Sensorless Brushless DC (BLDC) Motor Drives

by

Jianwen Shao

Thesis submitted to the Faculty of the

Virginia Polytechnic Institute and the State University

in partial fulfillment of the requirements for the degree of

MASTER OF SCIENCE

in

Electrical Engineering

Approved by: _____

Dr. Fred C. Lee

_____ _____

Dr. Alex Q. Huang Dr. Fred Wang

September, 2003
Blacksburg, Virginia

Key Words: Sensorless BLDC drive, direct back EMF sensing, start-up

Direct Back EMF Detection Method for Sensorless Brushless DC (BLDC) Motor Drives

Jianwen Shao

ABSTRACT

Brushlesss dc (BLDC) motors and their drives are penetrating the market of home appliances, HVAC industry, and automotive applications in recent years because of their high efficiency, silent operation, compact form, reliability, and low maintenance.

Traditionally, BLDC motors are commutated in six-step pattern with commutation controlled by position sensors. To reduce cost and complexity of the drive system, sensorless drive is preferred. The existing sensorless control scheme with the conventional back EMF sensing based on motor neutral voltage for BLDC has certain drawbacks, which limit its applications.

In this thesis, a novel back EMF sensing scheme, direct back EMF detection, for sensorless BLDC drives is presented. For this scheme, the motor neutral voltage is not needed to measure the back EMFs. The true back EMF of the floating motor winding can be detected during off time of PWM because the terminal voltage of the motor is directly proportional to the phase back EMF during this interval. Also, the back EMF voltage is referenced to ground without any common mode noise. Therefore, this back EMF sensing method is immune to switching noise and common mode voltage. As a result, there are no attenuation and filtering necessary for the back EMFs sensing.

This unique back EMF sensing method has superior performance to existing methods which rely on neutral voltage information, providing much wider motor speed range at low cost.

Based on the fundamental concept of the direct Back EMF detection, improved circuitry for low speed /low voltage and high voltage applications are also proposed in the thesis, which will further expand the applications of the sensorless BLDC motor drives.

Starting the motor is critical and sometime difficult for a BLDC sensorless system. A practical start-up tuning procedure for the sensorless system with the help of a dc tachometer is described in the thesis. This procedure has the maximum acceleration performance during the start-up and can be used for all different type applications.

An advanced mixed-signal microcontroller is developed so that the EMF sensing scheme is embedded in this low cost 8-bit microcontroller. This device is truly SOC (system-on-chip) product, with high-throughput Micro core, precision-analog circuit, in-system programmable memory and motor control peripherals integrated on a single die. A microcontroller-based sensorless BLDC drive system has been developed as well, which is suitable for various applications, including hard disk drive, fans, pumps, blowers, and home appliances, etc.

Acknowledgment

I am greatly indebted and respectful to my advisor, Dr. Fred C Lee, for his guidance and support through the years when I was in CPES. His rigorous attitude to do the research and inspiring thinking to solve problems are invaluable for my professional career.

I'd like to express my heartfelt thanks to Dr. Alex Q. Huang, and Dr. Fred F. Wang for their time and efforts they spent as my committee members. I am also grateful for the help of CPES faculty and staff members, Dr. Dan Y. Chen, Terasa Shaw and Linda Galla.

I would like to give special thanks to Dr. Yilu Liu, Dr. Caisy Ho, Dr. Peter Lo, Dr. Y.A. Liu and Mr. Chuck Schumann for their encouragement during my difficult time.

I would like to appreciate my fellow graduate students in CPES. They are too many to mention, Mr. Xiukuan Jing, Dr. Xiaochuan Jia, Dr. Wei Dong, Mr. Dengming Peng, Mr. Yuqing Tang, Dr. Fengfeng Tao, Dr. Pit-Long Wong, Dr. Peng Xu, Mr. Kaiwei Yao, Dr. Qun Zhao, Mr. Huibin Zhu, and Dr. Lizhi Zhu. To me, the friendship between CPES members is a big treasure. Their hardworking, perseverance, sharing, and self-motivate are always amazing me.

My thanks also go to brothers and sisters in VT Chinese Bible Study Group and Blacksburg Chinese Christian Fellowship.

Last but not least, I would like to thank my wife, Lin Xie, for her consistent love, support, understanding, encouragement, and self-sacrifice, for the life we experienced together, both in our good time and hard time.

Table of Content

Table of Figures

List of Tables

Chapter I

Introduction

1.1 Background

Brushless dc (BLDC) motors have been desired for small horsepower control motors due to their high efficiency, silent operation, compact form, reliability, and low maintenance. However, the control complexity for variable speed control and the high cost of the electric drive hold back the widespread use of brushless dc motor. Over the last decade, continuing technology development in power semiconductors, microprocessors/logic ICs, adjustable speed drivers (ASDs) control schemes and permanent-magnet brushless electric motor production have combined to enable reliable, cost-effective solution for a broad range of adjustable speed applications.

Household appliances are expected to be one of fastest-growing end-product market for electronic motor drivers (EMDs) over the next five years [1]. The market volume is predicted to be a 26% compound annual growth rate over the five years from 2000 to 2005 (See Fig.1.1). The major appliances in the figure include clothes washers, room air-conditioners, refrigerators, vacuum cleaners, freezers, etc. Water heaters, hot-water radiator pumps, power tools, garage door openers and commercial appliances are not included in these figures. Household appliance have traditionally relied on historical classic electric motor technologies such as single phase AC induction, including split phase, capacitor-start, capacitor–run types, and universal motor. These classic motors typically are operated at constant-speed directly from main AC power without regarding

the efficiency. Consumers now demand for lower energy costs, better performance, reduced acoustic noise, and more convenience features. Those traditional technologies cannot provide the solutions.

On the other hand, in recent year, the US government has proposed new higher energy-efficiency standards for appliance industry. In the near future, those standards will be imposed [2]. These proposals present new challenges and opportunities for appliance manufactures.

In the same time, automotive industry and HVAC industry will also see the explosive growth ahead for electronically controlled motor system, the majority of which will be of the BLDC type [3,4]. For example, at present, the fuel pump in a car is driven by a dc brushed motor. A brush type fuel pump motor is designed to last 6,000 hours because of limit lifetime of the brush. In certain fleet vehicles this can be expended in less than 1 year. A BLDC motor life span is typically around 15,000 hours, extending the life of the motor by almost 3 times. It is in the similar situation for the air-conditioning blower and engine-cooling fan.

It is expected that demanding for higher efficiency, better performance will push industries to adopt ASDs with faster pace than ever. The cost effective and high performance BLDC motor drive system will make big contribution for the transition.

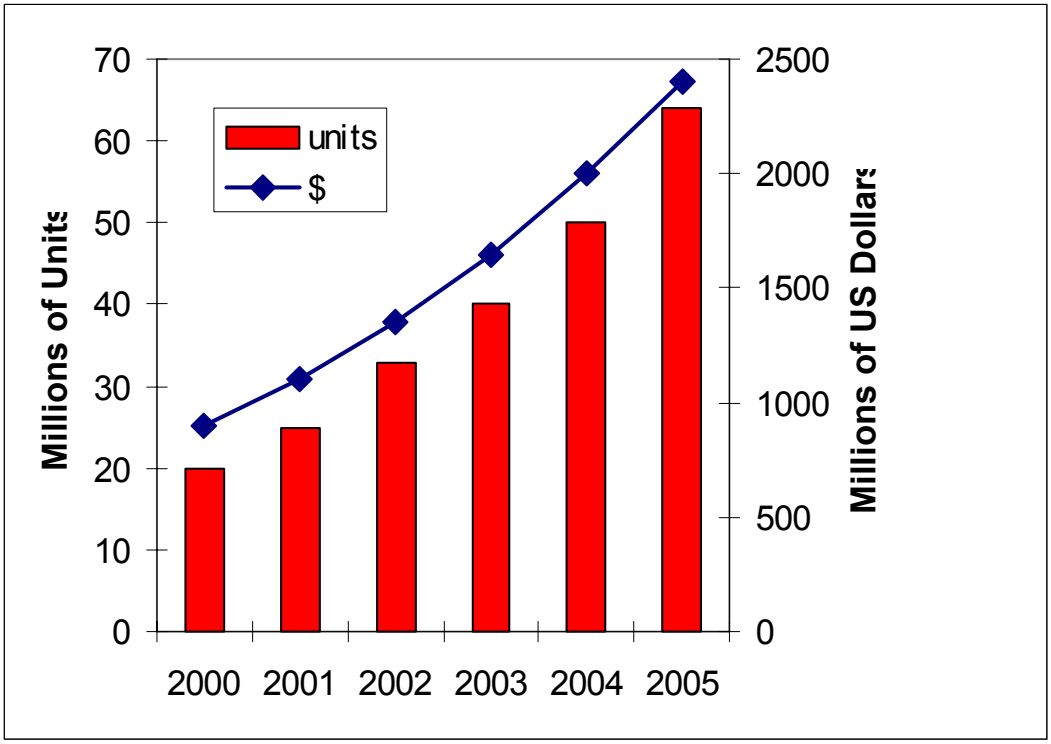

Fig.1. 1 Worldwide Market for electronic motor drives in household appliances.

1.2 Brushless DC (BLDC) Motors and Sensorless Drives

Brushless dc motor [5] is one kind of permanent magnet synchronous motor, having permanent magnets on the rotor and trapezoidal shape back EMF. The BLDC motor employs a dc power supply switched to the stator phase windings of the motor by power devices, the switching sequence being determined from the rotor position. The phase current of BLDC motor, in typically rectangular shape, is synchronized with the back EMF to produce constant torque at a constant speed. The mechanical commutator of the brush dc motor is replaced by electronic switches, which supply current to the motor windings as a function of the rotor position. This kind of ac motor is called brushless dc motor, since its performance is similar to the traditional dc motor with commutators. Fig.1.2 shows the structure of a BLDC motor.

These brushless dc motors are generally controlled using a three-phase inverter, requiring a rotor position sensor for starting and for providing the proper commutation sequence to control the inverter. These position sensors can be Hall sensors, resolvers, or absolute position sensors. A typical BLDC motor control system with position sensors is shown in Fig.1.3. Those sensors will increase the cost and the size of the motor, and a special mechanical arrangement needs to be made for mounting the sensors. These sensors, particularly Hall sensors, are temperature sensitive, limiting the operation of the motor to below about 75^{o}C [6]. On the other hand, they could reduce the system reliability because of the components and wiring. In some applications, it even may not be possible to mount any position sensor on the motor. Therefore, sensorless control of BLDC motor has been receiving great interest in recent years.

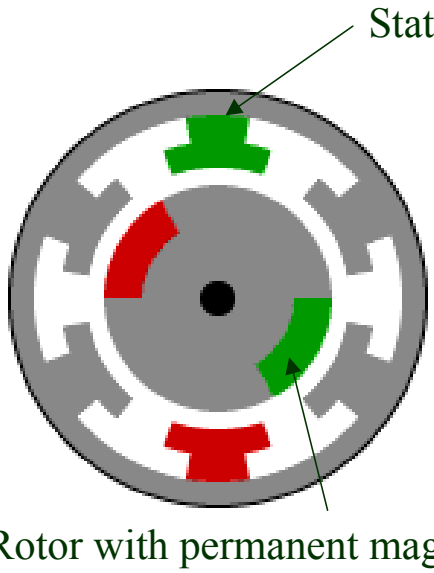

(A) Cross-section view of a brushless dc motor

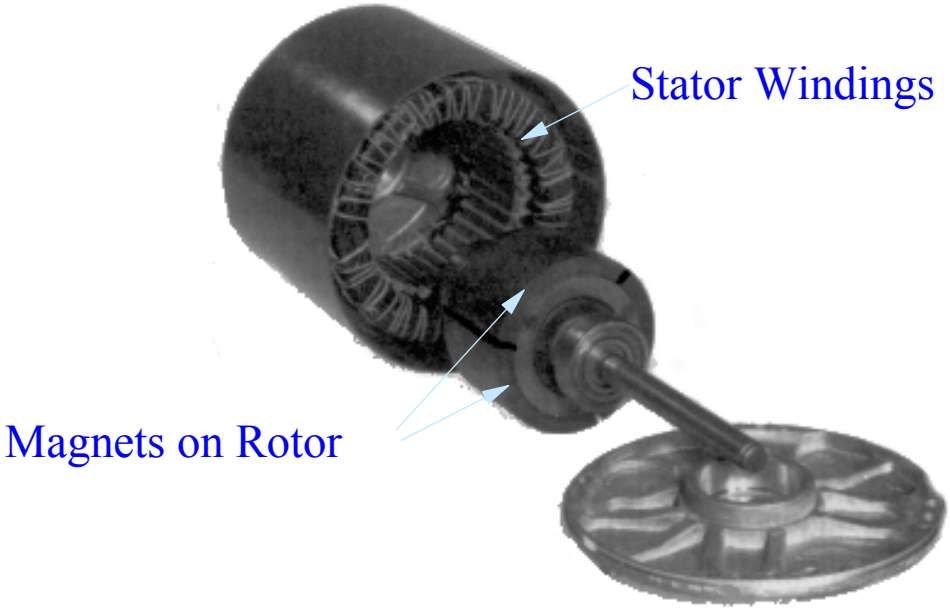

(B) A picture of a brushless dc motor

Fig.1. 2 Structure of a brushless dc motor

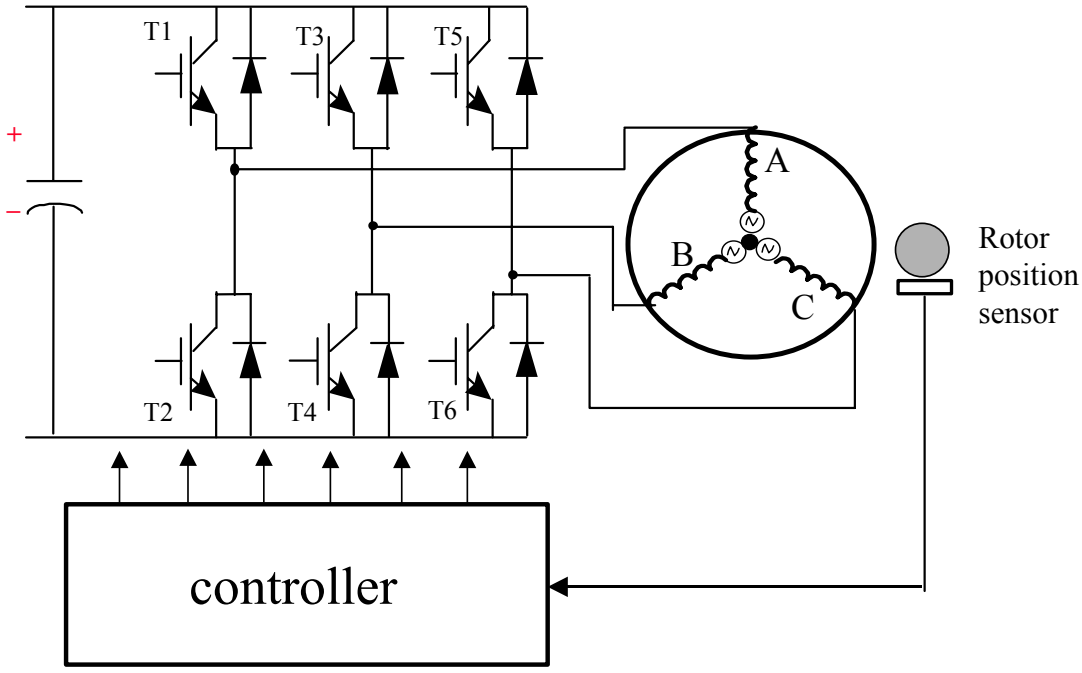

(A)

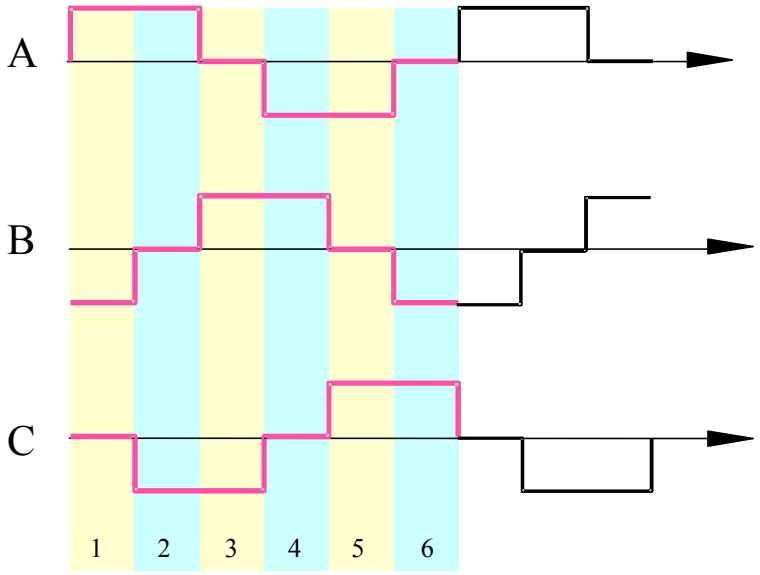

(B)

Fig.1. 3 (A) Typical brushless dc motor control system; (B). Typical three phase current waveforms in the BLDC motor.

Typically, a Brushless dc motor is driven by a three-phase inverter with, what is called, six-step commutation. The conducting interval for each phase is 120^o by electrical angle. The commutation phase sequence is like AB-AC-BC-BA-CA-CB. Each conducting stage is called one step. Therefore, only two phases conduct current at any time, leaving the third phase floating. In order to produce maximum torque, the inverter should be commutated every 60^o so that current is in phase with the back EMF. The commutation timing is determined by the rotor position, which can be detected by Hall sensors or estimated from motor parameters, i.e., the back EMF on the floating coil of the motor if it is sensorless system.

Basically, two types of sensorless control technique can be found in the literature [5,6]. The first type is the position sensing using back EMF of the motor, and the second one is position estimation using motor parameters, terminal voltages, and currents. The second type scheme usually needs DSPs to do the complicated computation, and the cost of the system is relatively high. So the back EMF sensing type of sensorless scheme is the most commonly used method, which is the topic of this thesis.

In brushless dc motor, only two out of three phases are excited at one time, leaving the third winding floating. The back EMF voltage in the floating winding can be measured to establish a switching sequence for commutation of power devices in the three-phase inverter. Erdman [7] and Uzuka [8] originally proposed the method of sensing back EMF (will be referred to the conventional back EMF detection method in this thesis) to build a virtual neutral point that will, in theory, be at the same potential as the center of a Y wound motor and then to sense the difference between the virtual

neutral and the voltage at the floating terminal. However, when using a chopping drive, the neutral is not a standstill point. The neutral potential is jumping from zero up to near dc bus voltage, creating large common mode voltage since the neutral is the reference point. Meanwhile, the PWM signal is superimposed on the neutral voltage as well, inducing a large amount of electrical noise on the sensed signal. To sense the back EMF properly, it requires a lot of attenuation and filtering. The attenuation is required to bring the signal down to the allowable common mode range of the sensing circuit, and the low pass filtering is to smooth the high switching frequency noise. Filtering causes unwanted delay in the signal. The result is a poor signal to noise ratio of a very small signal, especially at start-up where it is needed most. Consequently, this method tends to have a narrow speed range and poor start up characteristics. To reduce the switching noise, the back EMF integration [9] and third harmonic voltage integration [10] were introduced. The integration approach has the advantage of reduced switching noise sensitivity. However, they still have the problem of high common voltage in the neutral. An indirect sensing of zero crossing of phase back EMF by detecting conducting state of free-wheeling diodes in the unexcited phase was presented in [11]. The implementation of this method is complicated and costly, while its low speed operation is still a problem.

My colleague Jean-Marie Bourgeois [18] proposed an idea of a novel back EMF detection method, which does not require the motor neutral voltage. The true back EMF can be detected directly from terminal voltage by properly choosing the PWM and sensing strategy. The PWM signals are only applied to high side switches and the back EMF is detected during PWM off time. The resulting feedback signal is not attenuated or filtered, providing a timely signal with a very good signal/noise ratio. As a result this

sensorless BLDC driver can provide a much wider speed range, from start-up to full speed, than the conventional approaches mentioned above.

The work of this thesis conducts the theoretical analysis of the concept of the novel direct back EMF detection scheme presented in [18], providing full understanding of the method. Several problems or limitations of the scheme in different applications are found and analyzed. Based on the analysis, the causes for the problems are identified, and improvements are proposed, which are verified by real applications.

In the past, several integrated circuits based on neutral voltage construction have been commercialized [12][13][14]. Unfortunately, all these ICs are all analog devices, which lack flexibility in applications, regardless of poor performance at low speed. DSPs can apply very complicated control theory and speed estimation for the sensorless BLDC motor control. However, the cost of DSP is still relatively high. 8-bit microcontrollers have been the mainstay of embedded-control systems for a long time. The devices are available for a low cost; and the instructions sets are easy to use. Low system cost and high flexibility are good motivations to design a new microcontroller which is dedicated to sensorless BLDC drive. As a result, a low cost mixed signal microcontroller is developed, implementing the proposed back EMF sensing scheme.

This thesis is arranged as following. Chapter II briefly analyzes some back EMF detection schemes first. After analyzing problems associated with those schemes, the novel back EMF zero crossing detection is presented. A hardware implementation is introduced as well, and a low cost mixed-signal dedicated 8-bit microcontroller is

developed. Chapter III presents improved back EMF sensing schemes, extending the scheme to very low speed/low voltage applications and high voltage applications. Real application examples are also provided in Chapter II and Chapter III respectively. Chapter IV describes the starting algorithm for the sensorless BLDC system, a practical tuning procedure to start the motor with the best starting performance. Finally, Chapter V concludes the thesis and future research works are also suggested.

Chapter II

Direct Back EMF Detection for Sensorless BLDC Drives

In this chapter, a brief review of the conventional back EMF detection will be given first. Then, the proposed novel back EMF detection will be described. Experiment results demonstrate the advantages of the novel back EMF sensing scheme and the sensorless system. Specially, a low cost mixed-signal microcontroller that is the first commercial one dedicated for sensorless BLDC drives is developed, integrating the detection circuit and motor control peripherals with the standard 8-bit microcontroller core.

2.1 Conventional Back EMF Detection Schemes

For three-phase BLDC motor, typically, it is driven with six-step 120 degree conducting mode. At one time instant, only two out of three phases are conducting current. For example, when phase A and phase B conduct current, phase C is floating. This conducting interval lasts 60 electrical degrees, which is called one step.

A transition from one step to another different step is called commutation. So totally, there are 6 steps in one cycle. As shown in Fig.1.2B in previous chapter, the first step is AB, then to AC, to BC, to BA, to CA, to CB and then just repeats this pattern.

Usually, the current is commutated in such way that the current is in phase with the phase back EMF to get the optimal control and maximum torque/ampere. The commutation time is determined by the rotor position. Since the shape of back EMF

indicates the rotor position, it is possible to determine the commutation timing if the back EMF is known. In Fig.2.1, the phase current is in phase with the phase back EMF. If the zero crossing of the phase back EMF can be measured, we will know when to commutate the current.

As mentioned before, at one time instant, since only two phases are conducting current, the third winding is open. This opens a window to detect the back EMF in the floating winding. The concept detection scheme [5,6,7] is shown in Fig.2.2.

The terminal voltage of the floating winding is measured. This scheme needs the motor neutral point voltage to get the zero crossing of the back EMF, since the back EMF voltage is referred to the motor neutral point. The terminal voltage is compared to the neutral point, then the zero crossing of the back EMF can be obtained.

In most cases, the motor neutral point is not available. In practice, the most-commonly used method is to build a virtual neutral point that will, in theory, be at the same potential as the center of a Y wound motor and then to sense the difference between the virtual neutral and the voltage at the floating terminal. The virtual neutral point is built by resistors, which is shown in Fig 2.2 (B).

This scheme is quite simple. It has been used for a long time since the invention [6]. However, this scheme has its drawbacks.

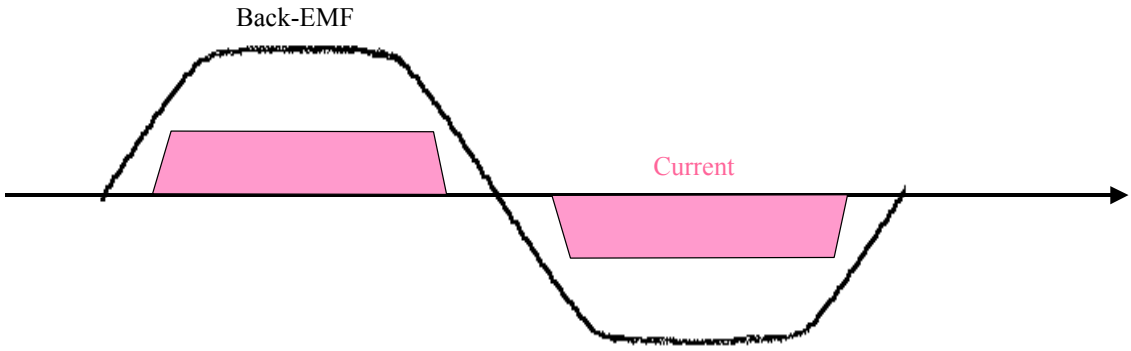

Fig.2.1 The phase current is in phase with the back EMF in brushless dc motor.

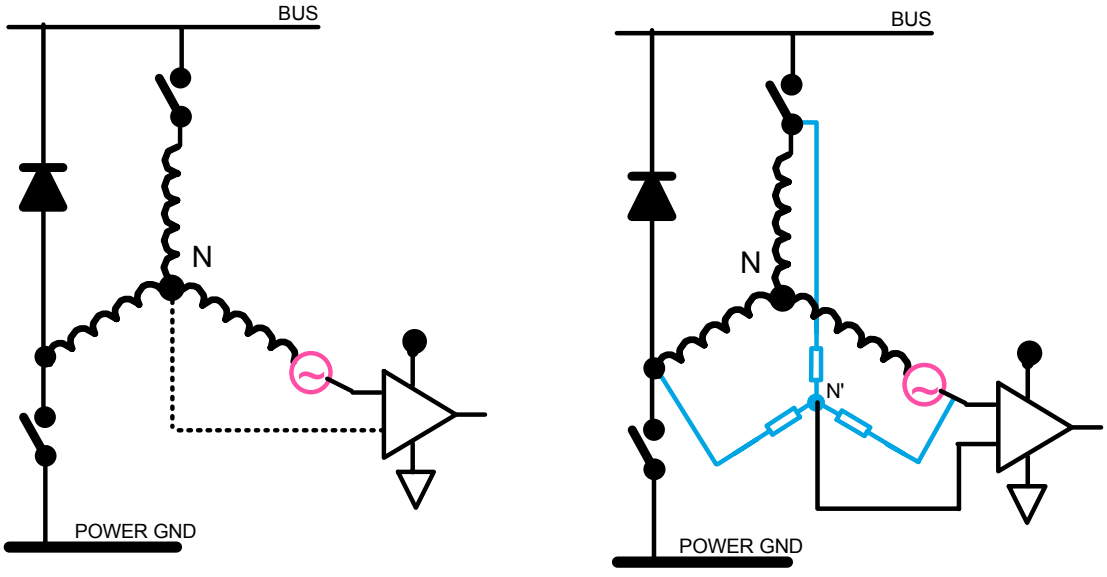

(A) (B)

Fig.2. 2 (A) Back EMF zero crossing detection scheme with the motor neutral point available; (B) back EMF zero crossing detection scheme with the virtual neutral point.

Because of the PWM drive, the neutral point is not a standstill point. The potential of this point is jumping up and down. It generates very high common mode voltage and high frequency noise. So we need voltage dividers and low pass filters to reduce the common mode voltage and smooth the high frequency noise, shown in Fig.2.3. For instance, if the dc bus voltage is 300 V, the potential of the neutral point can vary from zero to 300 V. The allowable common mode voltage for a comparator is typically a few volts, i.e. 5 V. We will know how much attenuation should be. Obviously, the voltage divider will reduce the signal sensitivity at low speed, especially at start-up where it is needed most. On the other hand, the required low pass filter will induce a fixed delay independent of rotor speed. As the rotor speed increases, the percentage contribution of the delay to the overall period increases. This delay will disturb current alignment with the back EMF and will cause severe problems for commutation at high speed. Consequently, this method tends to have a narrow speed range.

In the past, there have been several integrated circuits, which enabled sensorless operation of the BLDC, based on the scheme described above. These included Unitrode's UC3646, Microlinear's ML4425, and Silicon Systems's 32M595. All the chips have the drawbacks mentioned. Also, all of them are analog devices, which are lack of flexibility in applications.

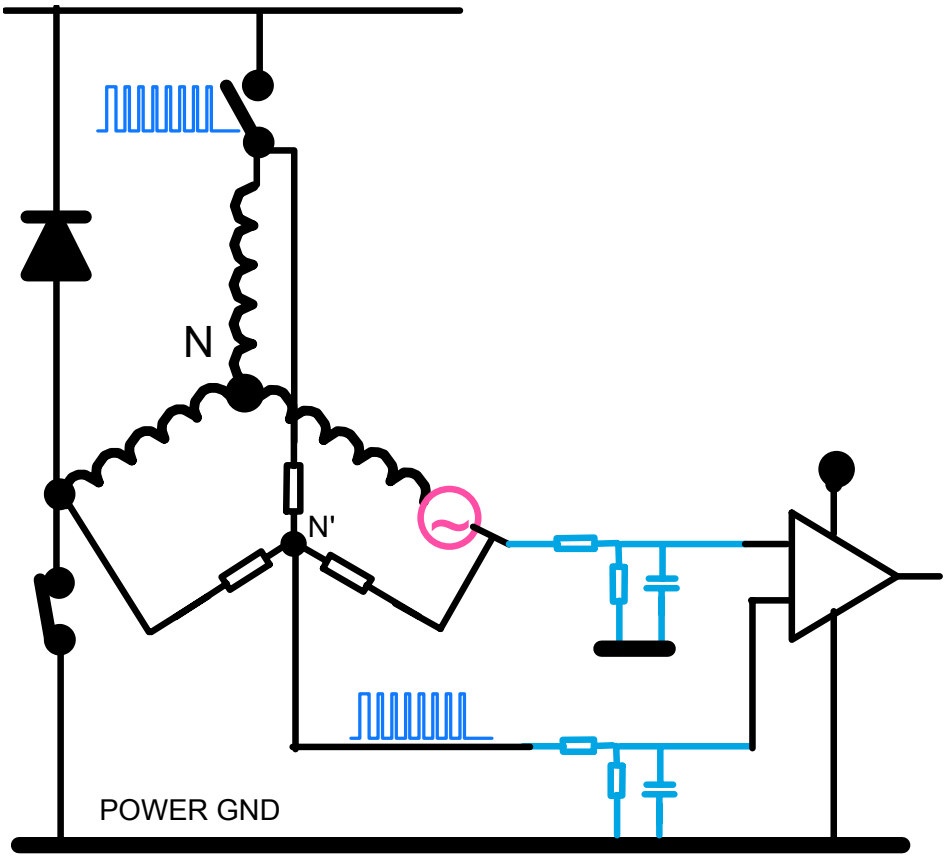

Fig.2. 3 Back EMF sensing based on virtual neutral point

A few other schemes for sensorless BLDC motor control were also reported in the literature.

The back EMF integration approach has the advantage of reduced switching noise sensitivity and automatically adjustment of the inverter switching instants to changes in the rotor speed [8]. The back EMF integration still has accuracy problems at low speeds.

The rotor position can be determined based on the stator third harmonic voltage component [9]. The main disadvantage is the relatively low value of the third harmonic voltage at low speed.

In [10], the rotor position information is determined based on the conducting state of free-wheeling diodes in the unexcited phase. The sensing circuit is relatively complicated and low speed operation is still a problem.

2.2 Proposed Direct Back EMF Detection Scheme

As described before, the noisy motor neutral point causes problems for the sensorless system. The proposed back EMF detection is trying to avoid the neutral point voltage. If the proper PWM strategy is selected, the back EMF voltage referred to ground can be extracted directly from the motor terminal voltage.

For BLDC drive, only two out of three phases are excited at any instant of time. The PWM drive signal can be arranged in three ways:

- On the high side: the PWM is applied only on the high side switch, the low side is on during the step.
- On the low side: the PWM is applied on the low side switch, the high side is on during the step.
- On both sides: the high side and low side are switched on/off together.

In the proposed scheme, the PWM signal is applied on high side switches only, and the back EMF signal is detected during the PWM off time. Fig2.4 shows the concept detection circuit. The difference between Fig2.4 and Fig2.2 is that the motor neutral voltage is not involved in the signal processing in Fig2.4.

Assuming at a particular step, phase A and B are conducting current, and phase C is floating. The upper switch of phase A is controlled by the PWM and lower switch of phase B is on during the whole step. The terminal voltage Vc is measured. Fig2.5 shows the PWM signal arrangement.

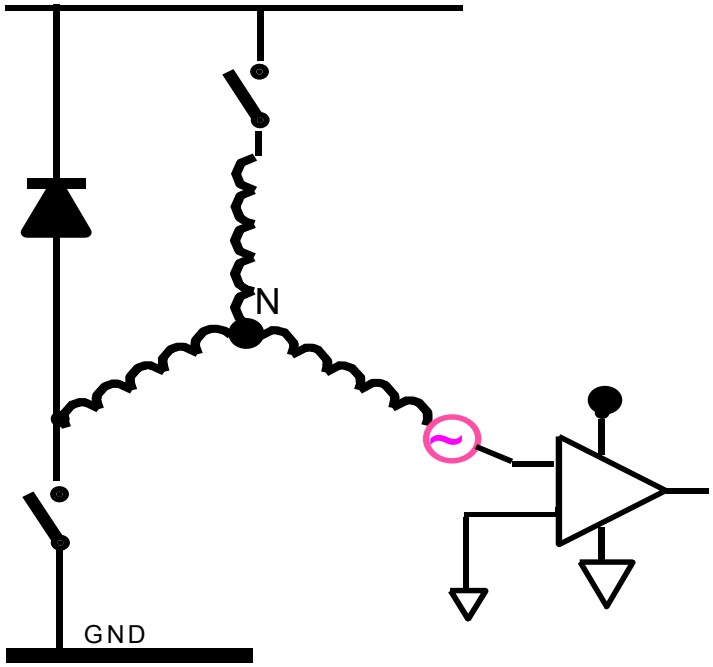

Fig.2. 4 Proposed back EMF zero crossing detection scheme.

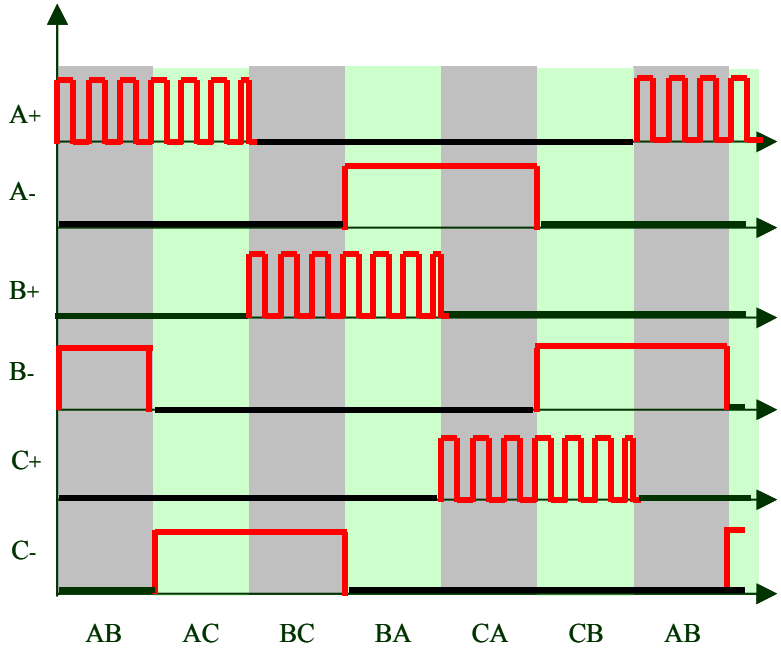

Fig.2. 5 Proposed PWM strategy for direct back EMF detection scheme

Fig2.6 shows the circuit model to conduct the analysis.

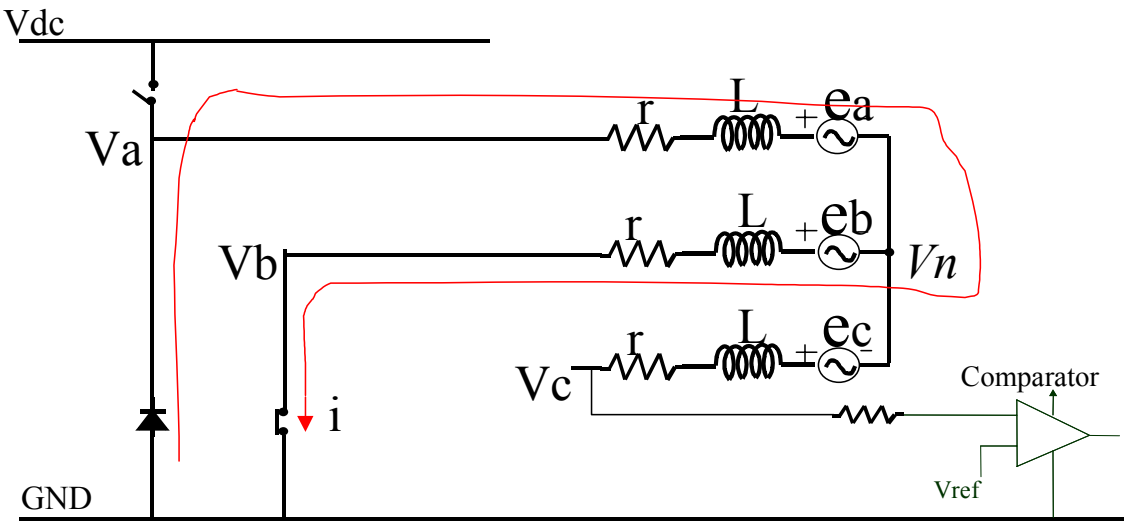

Fig.2. 6 Circuit model of proposed Back EMF detection during the PWM off time moment.

When the upper switch of phase A is turned on, the current is flowing through the switch to winding A and B. When the upper transistor of the half bridge is turned off, the current freewheels through the diode paralleled with the bottom switch of phase A. During this freewheeling period, the terminal voltage Vc is detected as Phase C back EMF when there is no current in phase C.

From the circuit, it is easy to see $v_c = e_c + v_n$, where Vc is the terminal voltage of the floating phase C, e_c is the phase back EMF and Vn is the neutral voltage of the motor.

From phase A, if the forward voltage drop of the diode is ignored, we have

$$v_n = 0 - ri - L\frac{di}{dt} - e_a \qquad (2.1).$$

From phase B, if the voltage drop on the switch is ignored, we have

$$v_n = ri + L\frac{di}{dt} - e_b \tag{2.2}$$

Adding (2.1) and (2.2), we get

$$v_n = -\frac{e_a + e_b}{2} \tag{2.3}$$

Assuming a balanced three-phase system, if we ignore the third harmonics, we have

$$e_a + e_b + e_c = 0 \tag{2.4}$$

Or, if we don't ignore the third harmonics, we will have

$$e_a + e_b + e_c = e_3 \tag{2.5}$$

where e_3 is the third harmonics.

Let's first finish the analysis without considering the third harmonics.

From (2.3) and (2.4),

$$v_n = \frac{e_c}{2} \tag{2.6}$$

So, the terminal voltage Vc,

$$v_c = e_c + v_n = \frac{3}{2}e_c \tag{2.7}$$

From the above equations, it can be seen that during the off time of the PWM, which is the current freewheeling period, the terminal voltage of the floating phase is directly proportional to the back EMF voltage without any superimposed switching noise. It is also important to note that this terminal voltage is referred to the ground instead of the

floating neutral point. So, the neutral point voltage information is not needed to detect the back EMF zero crossing, and we don't need to worry about the common mode voltage. Since the true back EMF is extracted from the motor terminal voltage, the zero crossing of the phase back EMF can be detected very precisely.

If we consider the third harmonics, from (2.3) and (2.5),

$$v_n = \frac{e_c}{2} - \frac{e_3}{2} \tag{2.8}$$

So, the terminal voltage Vc,

$$v_c = e_c + v_n = \frac{3}{2} e_c - \frac{e_3}{2} \tag{2.9}$$

Therefore, the terminal voltage will see the third harmonics. However, since the zero crossing of the fundamental wave will coincide with the zero crossing of the third harmonics, the third harmonic won't affect the zero crossing of the fundamental wave.

A few tests have been conducted to show the relationship between fundamental and third harmonics.

Fig2.7 and Fig2.8 show the test result for motor A. Fig2.9 and Fig2.10 show the result for motor B. The shapes of back EMF are different from two motors. Nevertheless, the zero crossing of the third harmonics is overlapping with that of fundamental for both motors, which means that the third harmonics will not affect the zero crossing of fundamental wave. For motor B, there is slightly unbalance for three phase. Even under

this situation, zero crossings of fundamental wave and third harmonic are still well overlapping.

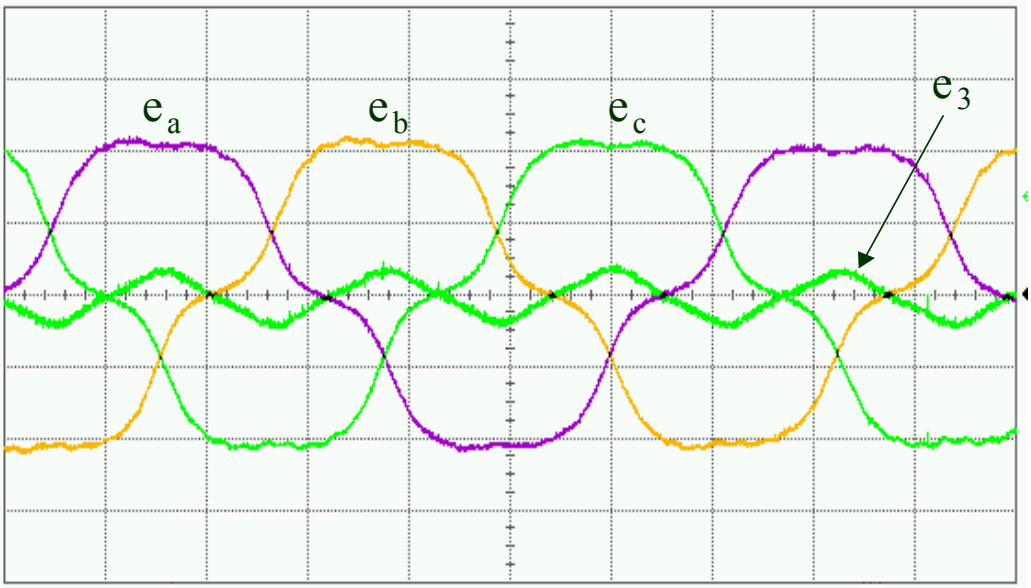

Fig. 2.7 Fundamental wave and third harmonics of back EMF for motor A

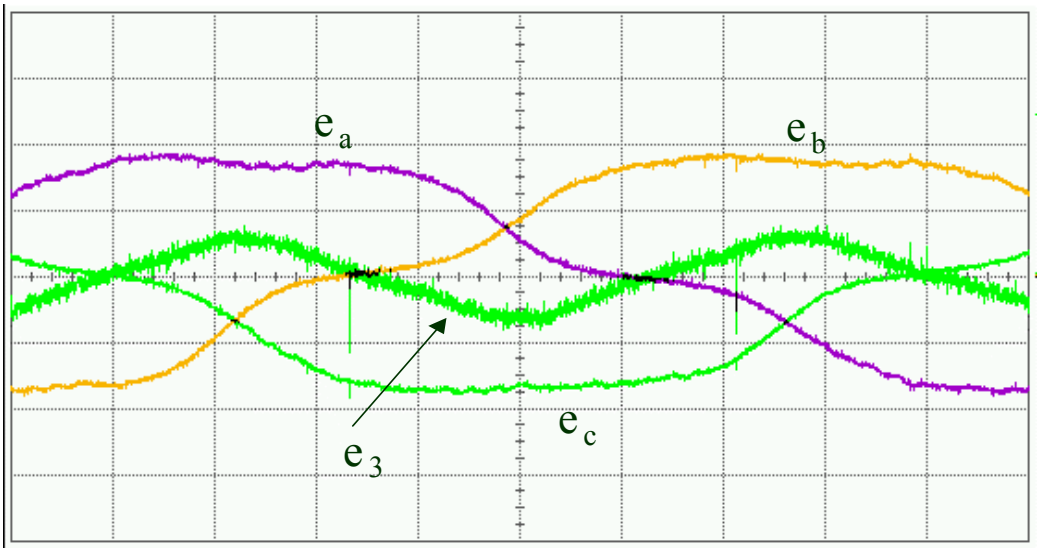

Fig.2. 8 Expanded waveform of Fundamental wave and third harmonics of back EMF for motor A

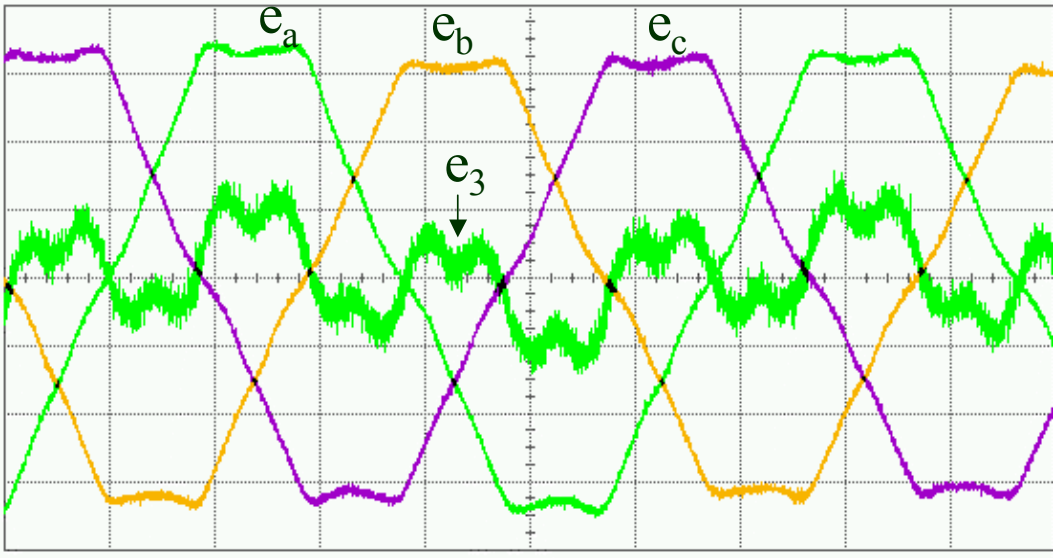

Fig. 2.9 Fundamental wave and third harmonics of back EMF for motor B

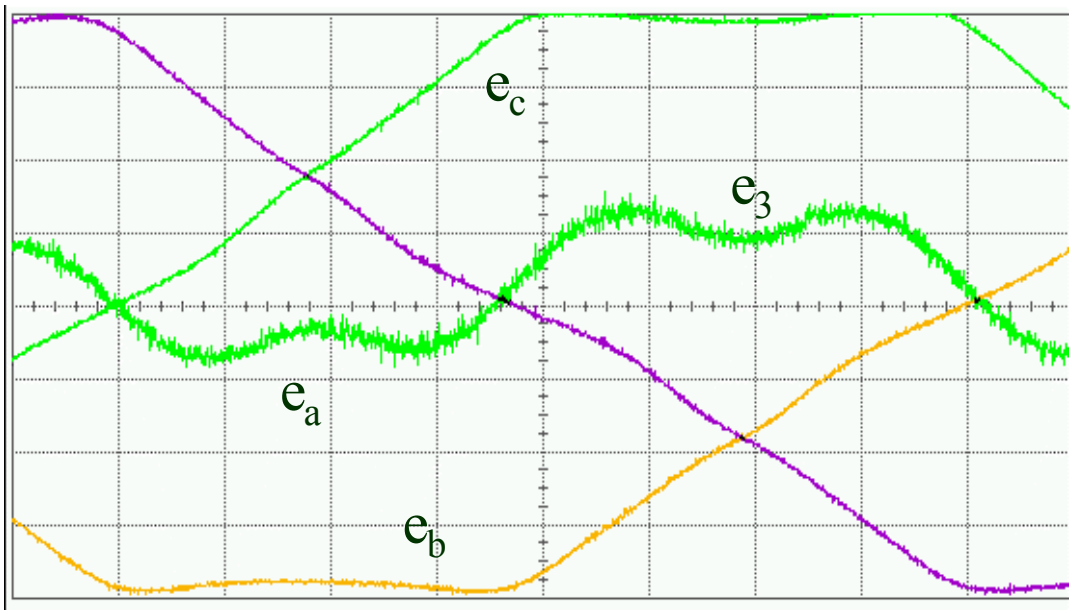

Fig.2. 10 Expanded waveform of Fundamental wave and third harmonics of back EMF for motor B

Therefore, we can neglect the third harmonics content in the terminal voltage for zero crossing detection. Equation 2.7 is valid for zero crossing detection purpose.

To illustrate the schema, Fig2.11 shows the terminal voltage waveform of the scheme. From this waveform, it is clear that the back EMF signal can be extracted from the terminal voltage when the phase is floating. From time T1 to T2, the winding is floating; from time T2 to T3, the winding is conducting; and from time T3 to T4, the winding is floating again. The back EMF signal can be detected when PWM is "off". If the back EMF is negative, it is clamped to about minus 0.7v by the diode paralleled with the switch in the inverter. When the back EMF is positive, it shows up in the terminal voltage.

Between time T1 and T2, rising edge of zero crossing is detected; and between T3 and T4, falling edge of the zero crossing can be detected.

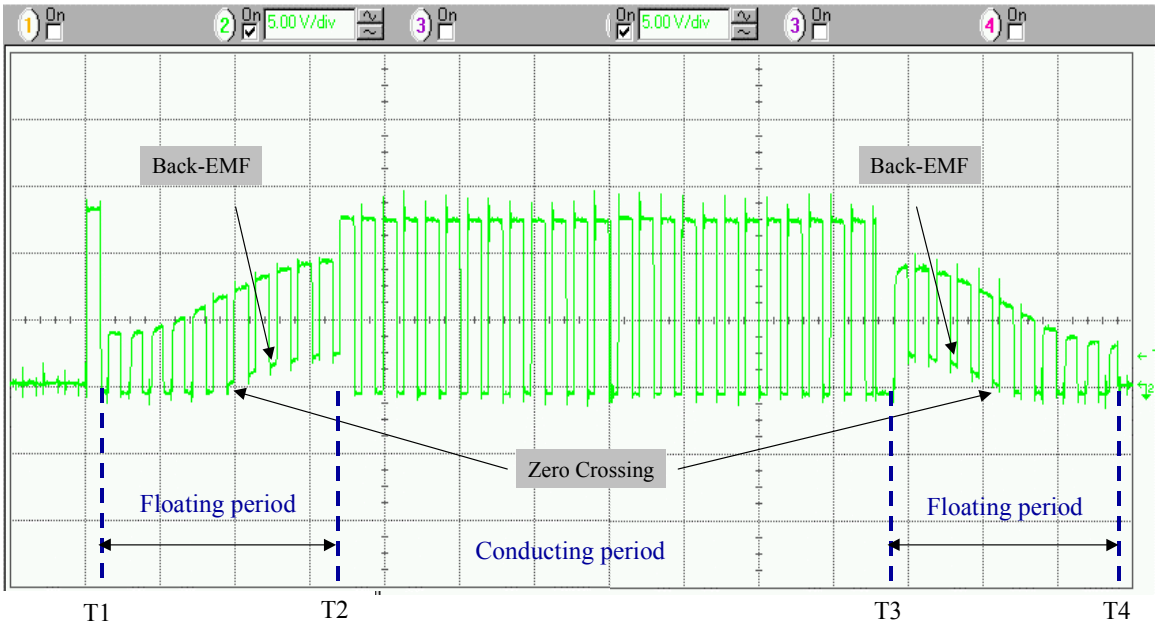

Fig.2. 11 Phase terminal voltage and the back EMF waveform.

As a summary, several advantages of the proposed back EMF sensing technique over the conventional schemes can be listed as following:

1) It has high sensitivity. First, since we don't use voltage divider, there is no attenuation. It still has good resolution even at low speed operation. Second, the high frequency switching noise can be rejected because the back EMF is sampled during the PWM off time. The synchronous sampling can easily get rid of the switching noise. Third, because the back EMF is referenced to the ground now, the common mode voltage is minimized.

2) It is instant value because there is no filtering in the circuit, which will be good for high-speed operation.

3) This sensing technique can be easily used to either high voltage or low voltage systems without much effort to scale the voltage.

4) Fast motor start-up is possible because of precise back EMF zero crossing detection without attenuation.

5) It is simple and easy to implement, which will be discussed in the next section.

2.3 Hardware Implementation of the Proposed Back EMF Detection Scheme

The synchronous sampling circuit is developed to detect the back EMF zero crossing. In recent year, with the development of IC mixed-signal technology, SOC (system-on-chip) devices are feasible. Precision-analog, high-throughput processors and in-system-programmable memory and other peripherals can be integrated on a single die. SOC devices have many advantages, including lower system cost, reduced board space, and superior system performance and reliability. The 8-bit microcontroller has been the mainstay of embedded-control systems for nearly 20 years. The devices are available for a low cost; instruction sets are easy to use. As a result, the back EMF detection circuit is integrated with a standard ST7 family microcontroller core to become a low cost dedicated sensorless BLDC microcontroller.

Firstly, let's take a look of the implementation of the synchronous sampling of the back EMF zero crossing.

Fig2.12 shows the hardware implementation for the back EMF zero crossing detection. The back EMF signals go through a multiplexer, and the controller selects which input to be sensed according to the motor commutation stages. Since only the zero crossing is of interest, the peak voltage is clamped at 5v by diodes, thereby keeping the voltage within the range of the sensing amplifier. The selected signal is compared to a fixed voltage reference, which is close to zero. During the off time, the back EMF is compared with reference voltage. The rising edge of the PWM, at the beginning of the PWM on time, which is the end of "off" time, will latch the comparator output to capture the zero crossing information.

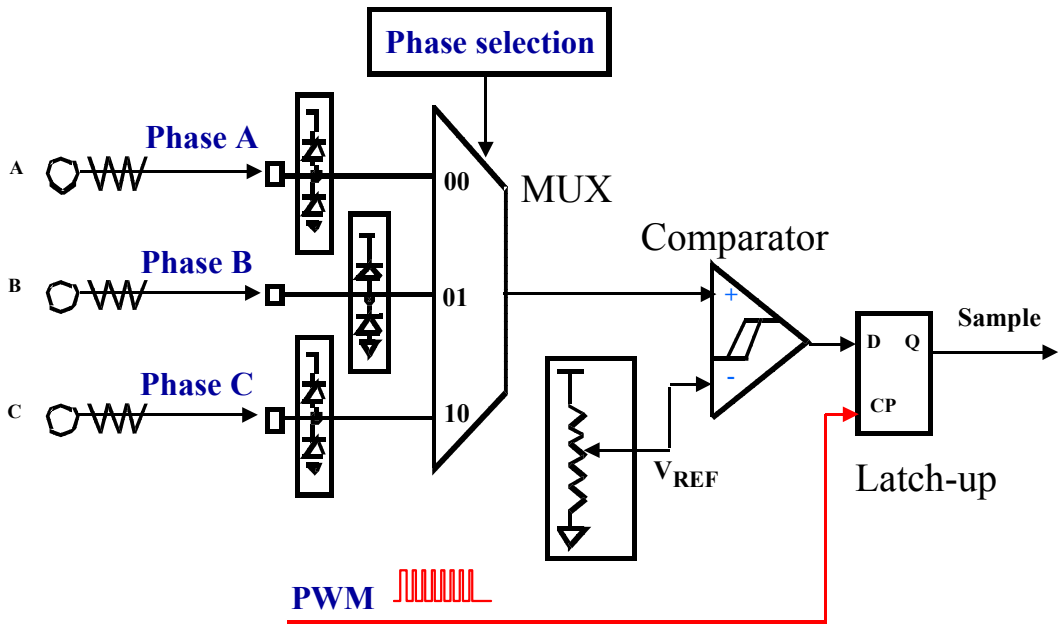

Fig.2.12. Synchronous sampling of the back EMF.

The proposed synchronous sampling circuit has been implemented in a hardware macro cell into a low cost 8-bit microcontroller ST72141 [11,13], which is dedicated to the sensorless BLDC driver. The block diagram of the hardware macro cell is shown in Fig.2.13. The Macro cell is split into four main parts.

- The back EMF Zero-Crossing Detector is the synchronous sampling circuit.
- The Delay Manager with a timer and an 8x8 bit hardware multiplier controls the proper delay from the zero crossing to commutation.
- The PWM Manager selects the control mode, current mode control or voltage mode control.

- The Channel Manager sends the PWM signals to right switches for six-step commutation.

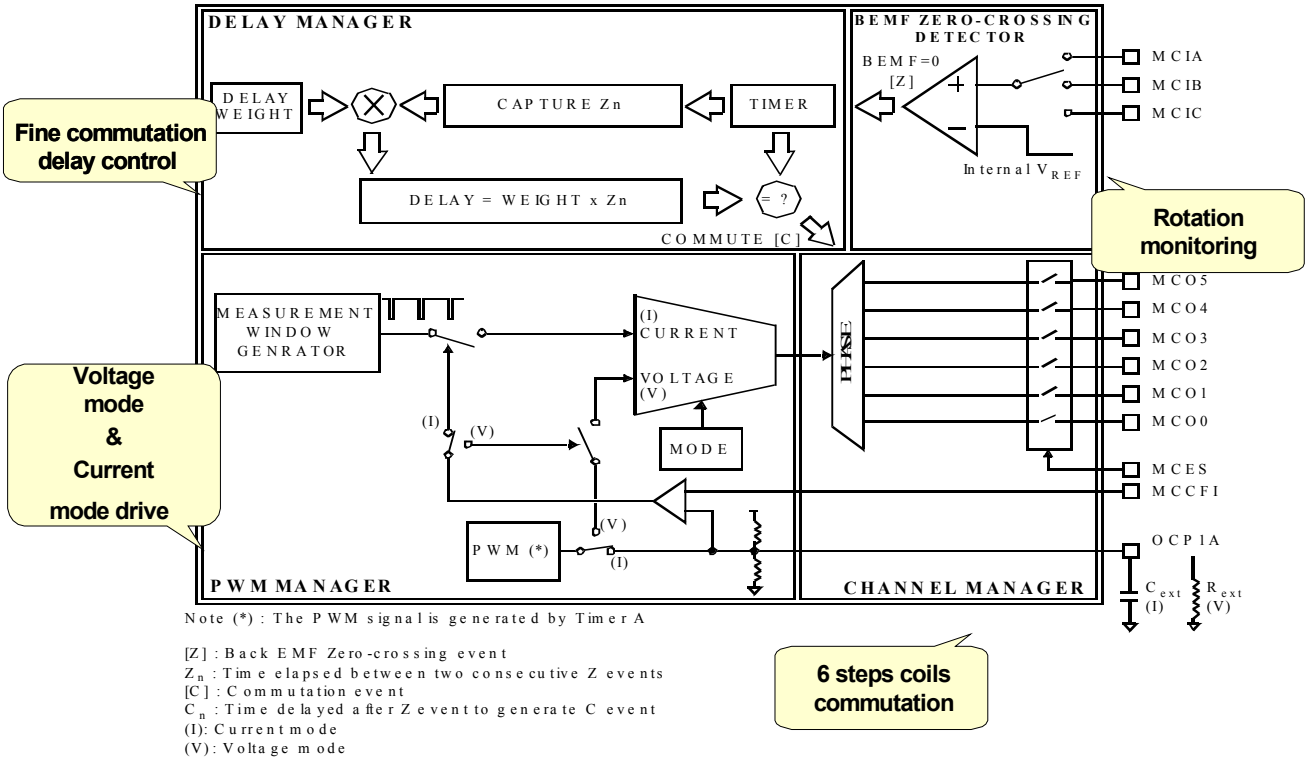

Fig.2. 13 Block diagram of the motor control hardware macro cell of ST72141.

The system schematic of the sensorless BLDC driver is drawn in Fig2.14. The motor terminal voltage is directly fed into the microcontroller through current limit resistors. For different voltage applications, we need to adjust the resistance value to set the right injected current.

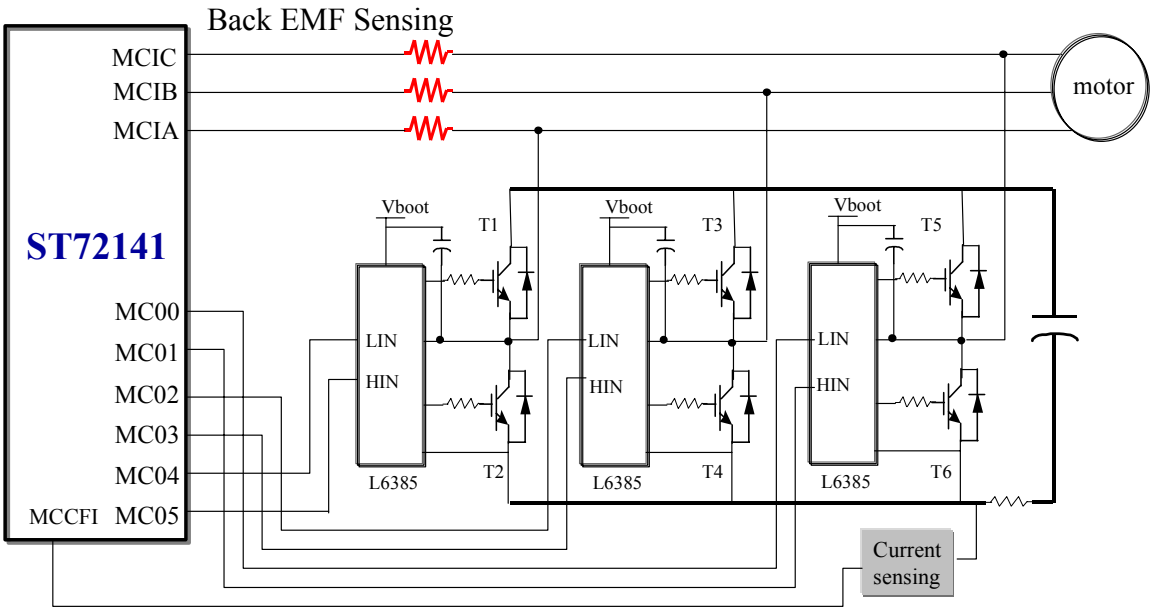

Fig.2. 14 The novel microcontroller-based sensorless BLDC motor driver.

This is the first commercial available dedicated microcontroller with the hardware macro cell for sensorless BLDC motor drives in the commercial market. Compared with other commercial analog I.C.s, the new microcontroller has superior performance with low cost and more flexibility and intelligence, which will be shown in an application example of automotive fuel pumps.

The commutation algorithm used is the standard BLDC control algorithm. The commutation will happen 30 electrical degrees after the back EMF zero crossing. Thanks to the programmability of the microcontroller, the system has much flexibility, running the motor in speed open loop or speed close loop depending on applications. Also it is

very convenient to adjust the control parameters. For example, the delay between the zero crossing and commutation can be easily adjusted by software. Usually, the delay from phase back EMF zero crossing to commutation is 30^{O} to keep the phase current in phase with phase back EMF. For some high-speed applications, commutation can be done in advance to have the field weakening effect to expand the speed range. The delay manager section in the hardware core does the delay adjustment controlled by software.

2.4 Key Experiment Waveforms

The proposed sensorless BLDC drive has been successfully applied to some home appliances for compressors, air blowers, and vacuum cleaner applications and automotive fuel pump and HVAC applications.

The following waveforms show some key operating waveforms of a sensorless BLDC drive system. Fig.2.15 shows the unclamped terminal voltage and back EMF waveforms. The phase back EMF of the floating winding is extracted from the winding terminal voltage during the PWM off time.

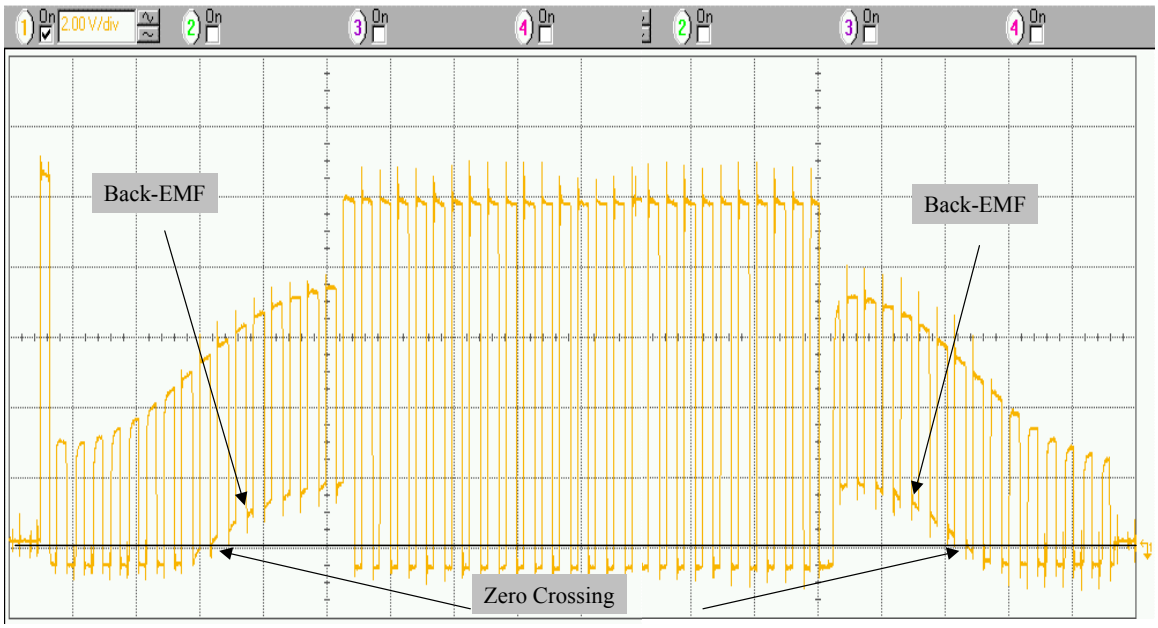

Fig.2. 15 Phase terminal voltage and back-EMF waveform.

Fig.2.16 shows the three phase terminal voltages, the back EMFs, and the zero-crossing signal. Each toggling edge of zero-crossing signal corresponds to the zero crossing of the back EMF.

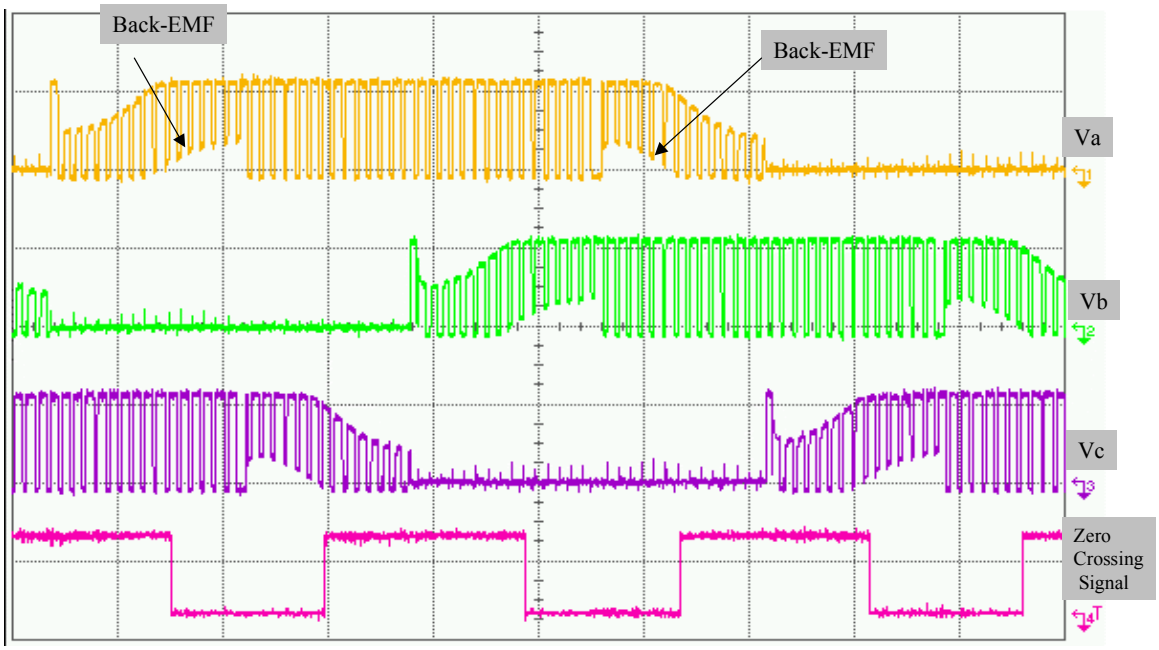

Fig.2. 16 Three phase back EMFs and the zero-crossings of back EMFs.

Fig.2.17 shows phase back EMF and the phase current. The sequence from back EMF zero crossing to commutation is clearly demonstrated. Approximitly, 30 electic degree after the zero crossing of the back EMF, the commutation will happen.

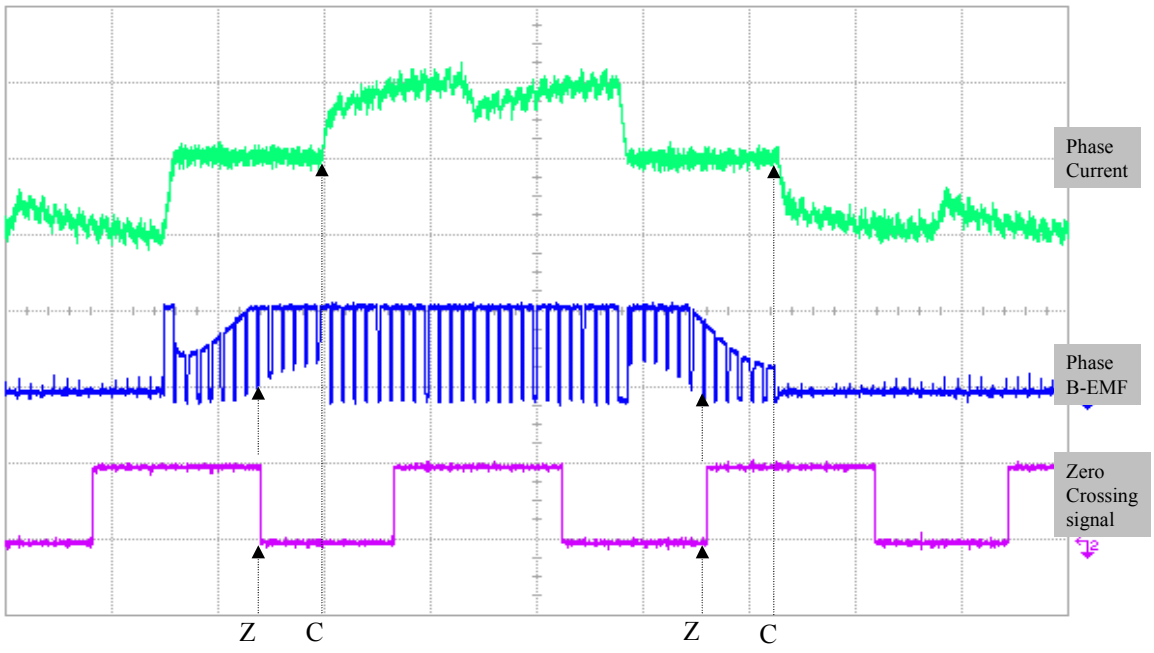

Fig.2.17 Sequence of zero crossing of back EMF and phase commutation.

As described before, this zero crossing detection has very good resolution even at low speed, when the amplitude of back EMF is low. Fig.2.18 shows the waveforms of back EMF and zero crossing signal at low motor speed. The system still can function very well even when the peak of back EMF is less than 1V.

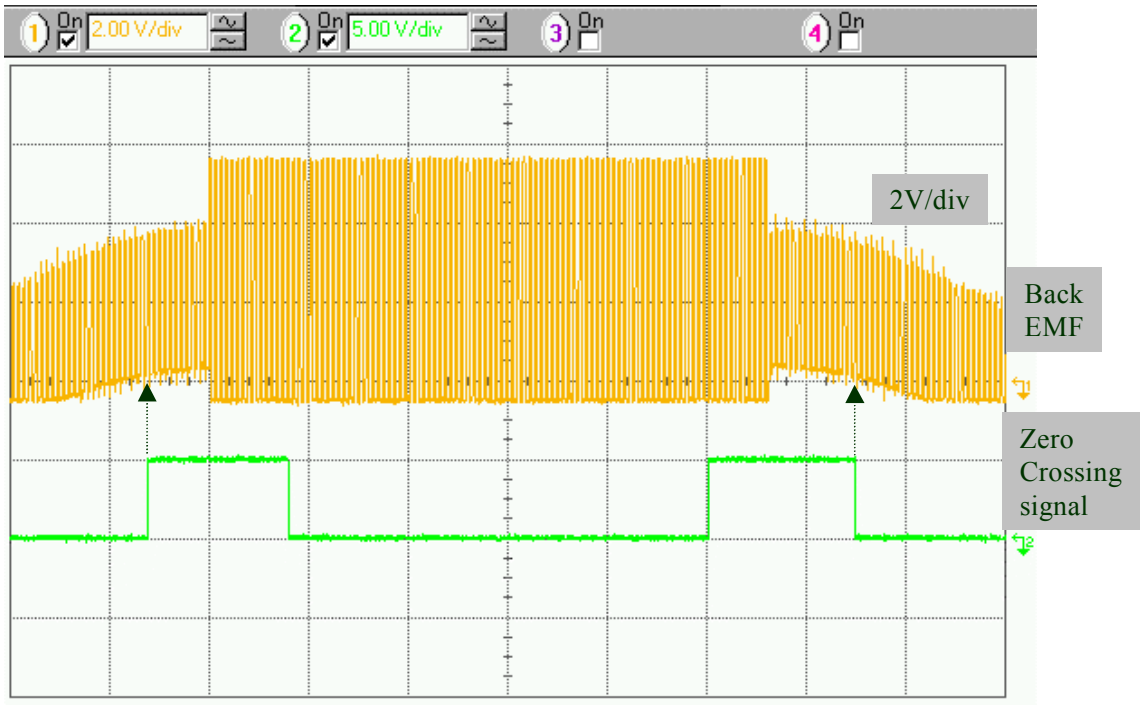

Fig.2.18 Back EMF and zero crossing at low speed operation.

If the speed needs to go further low, an improved circuit using OP AMP is developed to amplify the back EMF signal. The next chapter will discuss the improved circuit.

To evaluate the precision of zero crossing and the commutation timing, a motor with Hall sensors is driven with the sensorless scheme. Fig.2.19 shows the Hall sensor signals and the current commutation timing. The current commutation moment is aligned with the Hall sensor signals very well, which indicating the zero crossing detection is precise.

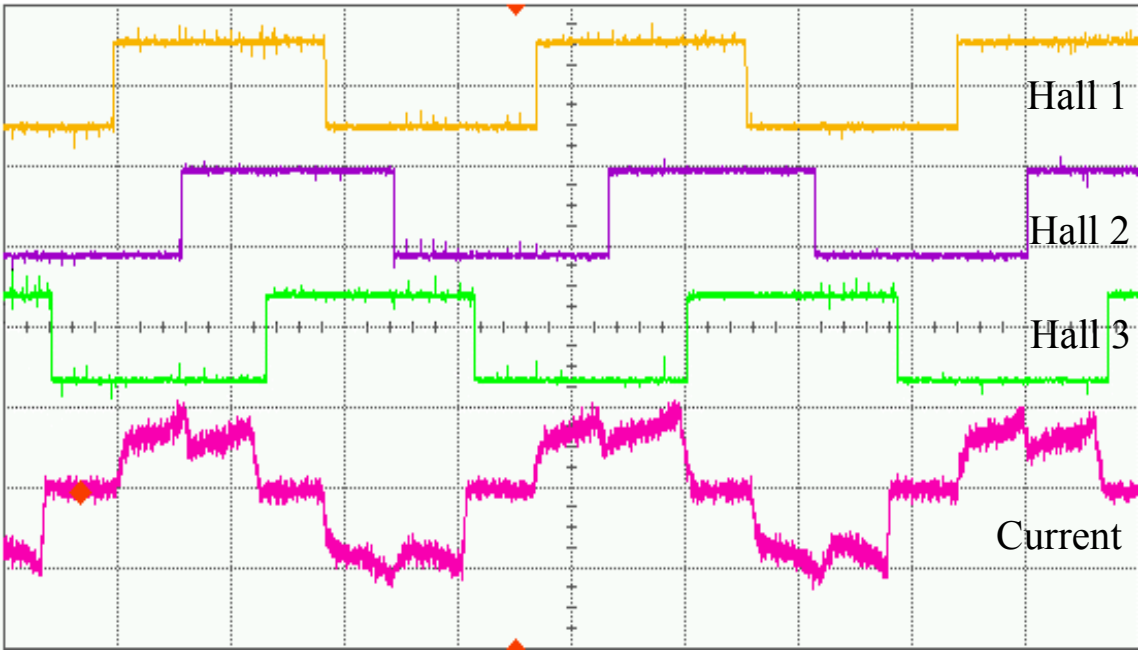

Fig.2.19 Hall sensor signals vs. the phase current.

For conventional method, it is difficulty to go to very high speed because of the delay caused by the low pass filter.

For the proposed direct back EMF detection method, the speed limitation is the sampling rate of back EMF signals since the back EMF is sampled at switching frequency F_s. The test results show that the sampling number of back EMF should be at least 3 in each step to have good resolution. So the maximum commutation frequency is $F_s/3$. As we know, there are 6 steps in one cycle. Therefore, the fundamental frequency is $F_s/18$. If the switching frequency is 18 KHz, the fundamental frequency is 1 KHz. If the motor is 4 poles motor, the maximum speed can be up to 30,000 rpm, which is fairly high speed operation. Fig2.20 shows a 4 poles motor is running at 30,000 rpm.

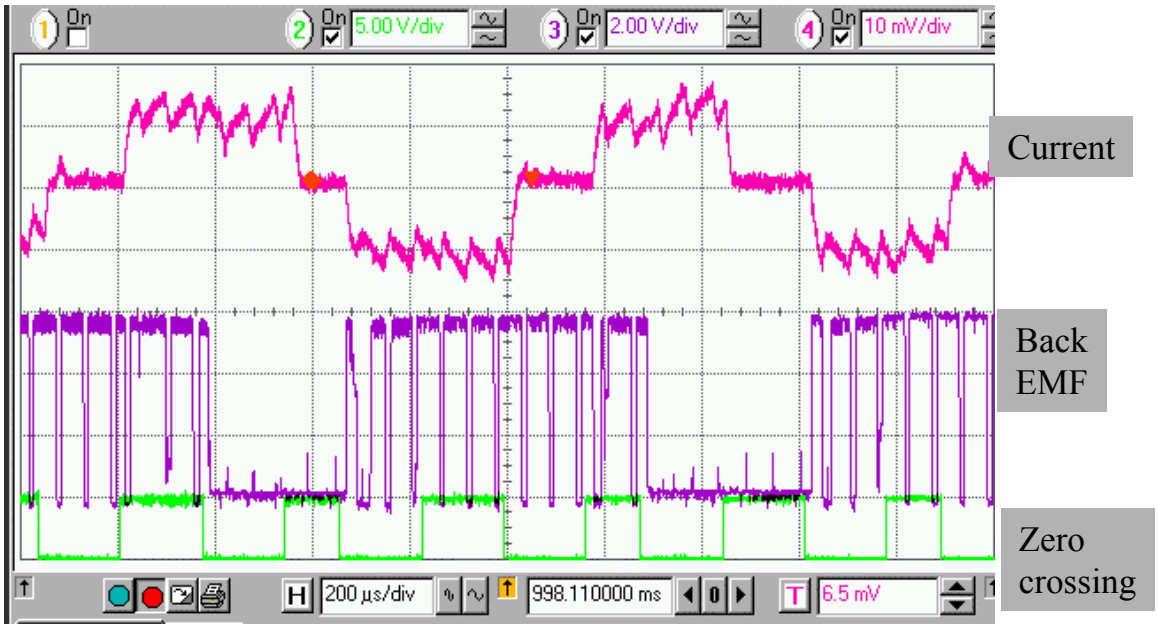

Fig.2. 20 High speed operation waveforms

2.5 An application Example: Automotive Fuel Pump

A brush type dc fuel pump motor is typically designed to last 6,000 hours. In certain fleet vehicles this can be expended in less than 1 year. A brushless dc motor life span is typically around 15,000 hours, extending the life of the motor by almost 3 times. Once a microcontroller is used to perform the brushless commutation other features can be incorporated into the application. Features such as electronic returnless fuel system control, fuel level processing, and fuel tank pressure sensing can be incorporated. These added features simplify the vehicle systems as well as drive overall cost down. Therefore, the fuel pump drive is a very good application for the proposed micro-controller based sensorless BLDC drive scheme [19].

The challenges of the automotive fuel pump application include:

1). Wide input operating voltage range from 6v ~24v. The issue is that how to make the system work at 6v input;

2) Fast and very reliable start-up of the motor within 200ms;

3). Interface Compatibility for speed command and communication;

4). Low cost.

Thanks to the unique back EMF sensing scheme and the flexibility brought by the microcontroller, all these issues are solved.

Fig2.21 shows the system block diagram for the sensorless drive system. The detailed schematic is in appendix 1.

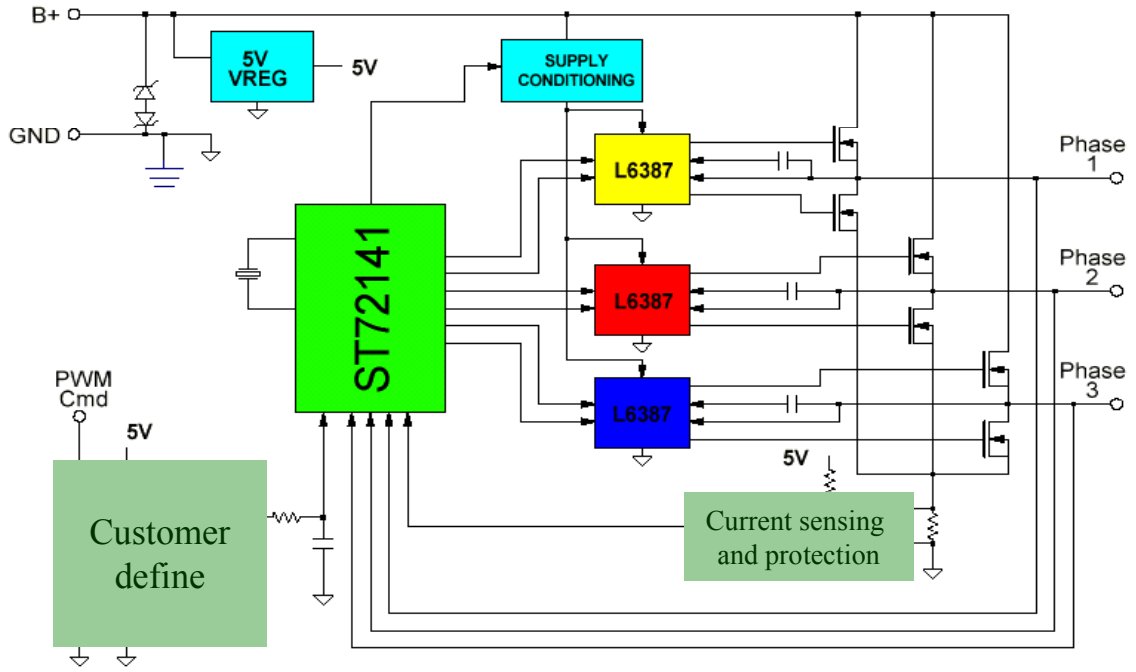

Fig.2. 21 System block diagram for the sensorless drive system of fuel pump.

The battery voltage can vary from 6v to 24v. At 6v, the gate driver will not function well. The minimum voltage for the gate driver chip L6387 is around 6.5v. A supply conditioning circuit, which is a simple charge pump circuit, is used to boost the voltage for the gate driver. Fig2.22 shows the supply conditioning circuit. The microcontroller will monitor the dc bus voltage (battery voltage). When the dc voltage is below certain threshold voltage (8v), the charge pump circuit will be activated. This supply conditioning circuit solves the wide voltage range issue.

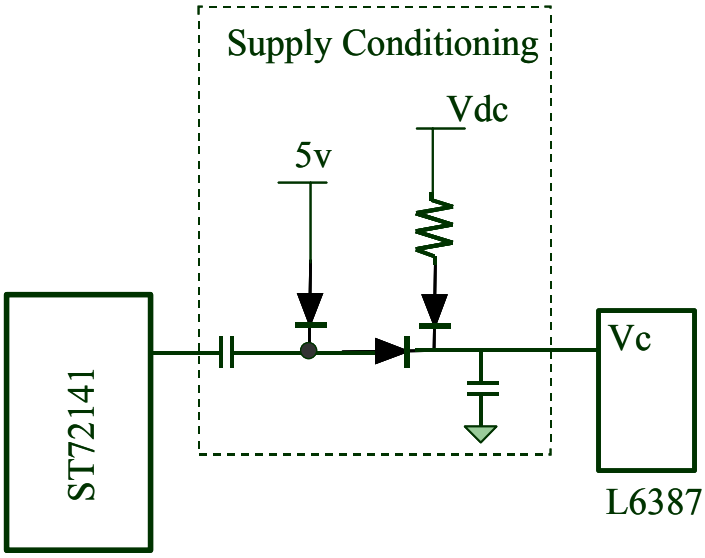

Fig.2. 22 Supply conditioning circuit foe fuel pump application.

The second issue is that the motor has to start quickly enough to build up the pressure when the engine is starting. With the conventional sensorless method, it is very difficult to start the motor very quickly. Thanks to the proposed high precision back EMF detection of the ST72141, quick starting of the BLDC motor can be accomplished.

When the motor is stop, there is no back EMF. Usually, the controller forces the motor to rotate with open loop commutation. The motor will try to accelerate the speed if the commutation frequency is increasing. After the motor generates enough back EMF, it switches to synchronous commutation, which is determined by the back EMF zero crossing.. Since we don't attenuate the back EMF signals, the controller can detect the back EMF zero crossing at lower speed. Therefore, the motor can finish start process

sooner than conventional method. Using this novel back EMF detection, it is possible to switch to synchronous commutation when the peak back EMF amplitude is as little as 0.5v.

Fig 2.23 shows a starting waveform of the pump. The fuel pump finishes the start-up within 150ms. How to achieve this best start-up will be discussed in the chapter IV.

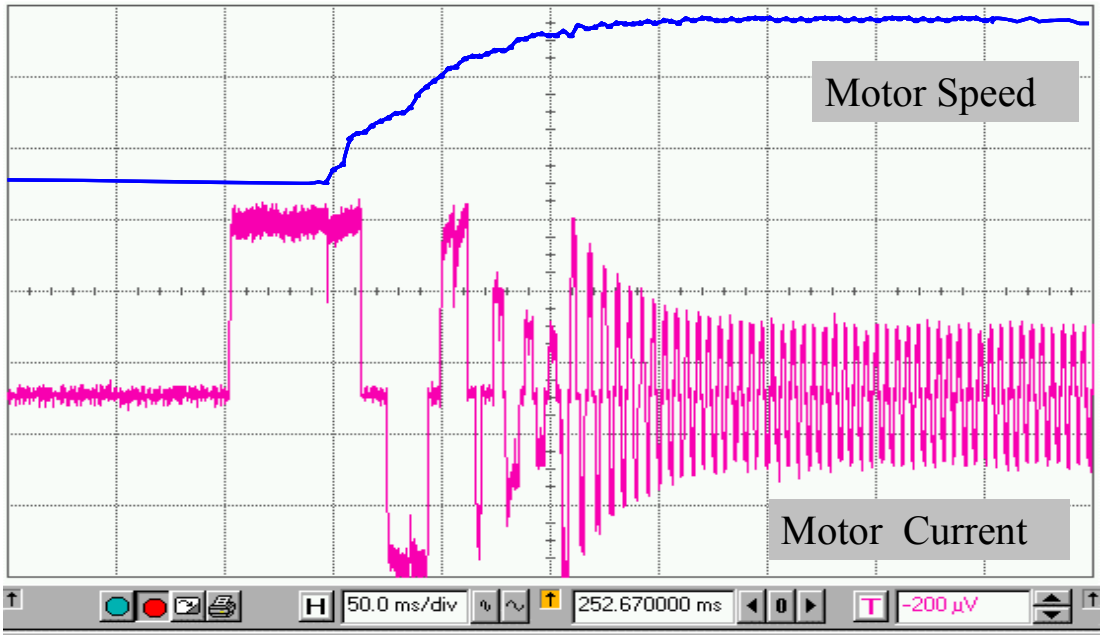

Fig.2. 23 Start-up waveforms of the fuel pump

The pump can be controlled either by pressure sensor or Powertrain Control Module (PCM). If it is controlled by pressure sensor, the motor speed will be regulated according to the feedback pressure sensor to maintain the desired fuel pressure. If it is controlled by PCM, the speed command will be PWM pulse train. The motor speed will directly follow

the duty cycle of the PWM signal from PCM. The microcontroller can easily identify the control mode and control the motor. The communication is relatively easy when there is a microcontroller in the system. Meanwhile, fuel level, fuel tank pressure, and fuel temperature can be monitored by the microcontroller as well. All these information can be sent back to Powertrain Control Module (PCM) through certain protocol. These monitoring functions are integrated in this Fuel Pump Driver Module (FPDM). The integration reduces over all system cost. The schematic is shown in appendix 1.

2.6 Summary

A novel back EMF sensing technique without motor neutral voltage for BLDC drives is presented in this chapter. The true back EMF can be synchronously detected during off time of PWM because the terminal voltage of the motor is directly proportional to the phase back EMF during this interval. This back EMF sensing method is immune to switching noise by synchronous sampling. Also, the back EMF information is referred to ground without any common mode noise. Therefore, This unique back EMF sensing method has superior performance to others which rely on neutral voltage information, providing much wider motor speed range with low cost. Even though the back EMF signal may contain high order harmonics, it will not affect the zero crossing detection.

Furthermore, this back EMF sensing scheme is embedded in a low cost microcontroller. This microcontroller integrates the analog detection circuit and other peripherals for motor control with a standard micro core, reducing the total system cost.

The test results verify the analysis and demonstrate the advantages of this novel back EMF detection scheme and mixed-signal microcontroller system. An example application of this microcontroller-based sensorless BLDC drive system is described in the chapter. The applications of this sensorless BLDC can include hard disk drive, fans, pumps, blowers, and home appliances, etc.

Chapter III

Improved Circuits for Direct Back EMF Detection

The back EMF detection method described in chapter II has to have minimum PWM off time. Therefore, it cannot go to 100% duty cycle. For some applications, the dc bus is low, like automotive applications. The bus voltage utilization is very important. An alternate back EMF detection is proposed in the chapter to solve the duty cycle limit problem.

For some applications, if the motor speed goes very low, the amplitude of the back EMF can be very low. In chapter II, Fig.2.18 shows a waveform when the amplitude of the back EMF is low. We find that the zero crossing is not evenly distributed. Theoretically, the zero crossing will happen every 60 electrical degree, so they should be evenly distributed. The inaccurate zero detection can cause wrong commutation, which probably could stall the motor at heavy load. Also bad zero crossing detection will cause bad speed regulation for close loop control because the speed feedback is based on the zero crossing.

The major reason is voltage drop across the diode in the inverter, biasing the back EMF signals. Also, the threshold voltage of the zero crossing comparison contributes to the unsymmetrical phenomenon to some extend.

In this chapter, the reason causing the unsymmetrical zero crossing is analyzed and an improved circuit is presented.

In high voltage applications, an unexpected signal delay issue for this sensorless scheme is identified. An improved circuit for high voltage applications is presented in this chapter as well.

3.1 Back EMF Detection During PWM On Time

In chapter II, we describe the direct back EMF detection during PWM off time. A true back EMF signal can be captured during that interval. However, one limitation for that method is that it cannot go to 100% duty cycle since we need minimum off time to have the time window to detect the back EMF. For some applications, it is not desirable. Can we detect the back EMF during PWM on time such that we don't need that minimum off time?

We need to find out the terminal voltage signal during PWM on time for the floating phase. If phase A and B are conducting current, phase C is floating. The terminal voltage Vc is detected.

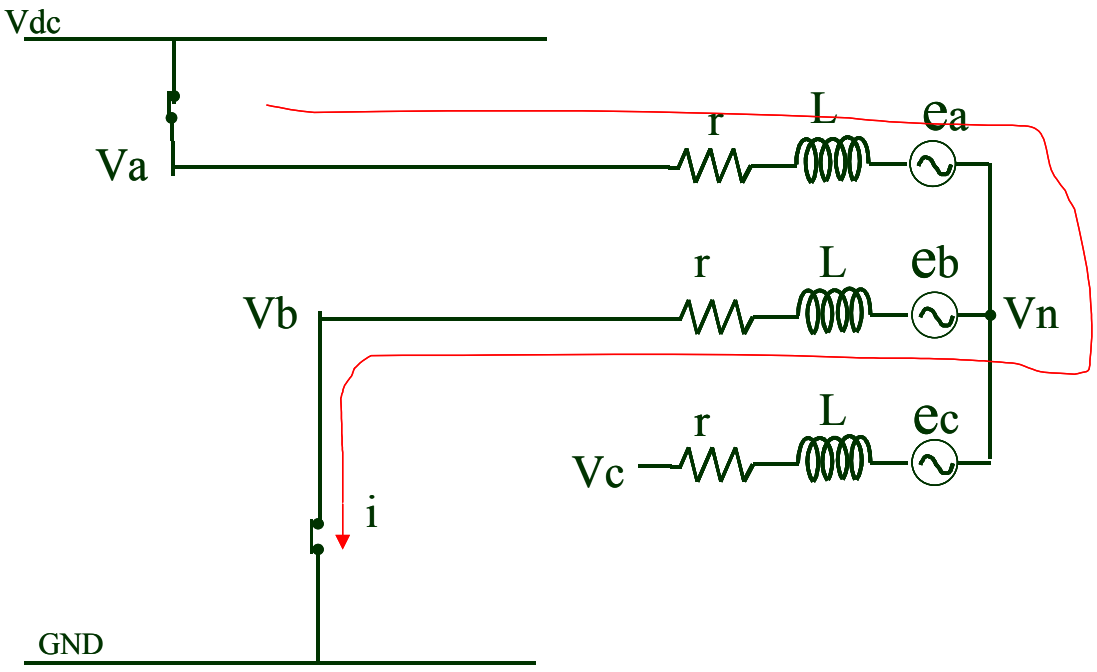

Fig.3. 1 Back EMF detection during the PWM on time

From phase A, we have

$$v_n = v_{dc} - v_{mos} - ri - L\frac{di}{dt} - e_a \qquad (3.1).$$

From phase B, we have

$$v_n = v_{mos} + ri + L\frac{di}{dt} - e_b \qquad (3.2).$$

Where Vd is the forward voltage drop of the diode, Vmos is the voltage drop on MOSFET.

From (3.1) and (3.2),

$$v_n = \frac{v_{dc}}{2} - \frac{e_a + e_b}{2} \qquad (3.3).$$

Also from the balance three-phase system, ignoring high order harmonics just like what we did in chapter II, we have

$$e_a + e_b + e_c = 0 \qquad (3.4).$$

From (3.3) and (3.4),

$$v_n = \frac{v_{dc}}{2} + \frac{e_c}{2} \qquad (3.5)$$

So, the terminal voltage Vc,

$$v_c = e_c + v_n = \frac{3}{2}e_c + \frac{v_{dc}}{2} \qquad (3.6).$$

From equation 3.6, the terminal voltage equals to back EMF plus the half of dc bus voltage. If we compare Vc with Vdc/2, then we can get the zero crossing of the back EMF. To reduce the common mode voltage, we need to attenuate the signal. Since we

only need to do this at high speed, the back EMF has high amplitude. The attenuation will not affect the sensitivity of the signal.

Therefore, if 100% duty cycle is necessary for some application, the back EMF detection can be done during PWM on time. At lower speed, the back EMF can be detected during off time. After the duty cycle is higher than certain level, the detection can be done during on time. The zero crossing reference changes to half of dc bus voltage, instead of ground.

This feature has been implemented into ST7MC, new version of ST72141 [25].

3.2 Improved Circuit for Low Speed/Low Voltage Applications

3.2.1 Biased Back EMF Signal

In the previous chapter, when we do the circuit analysis, we ignore the voltage drop in the diode and the switch. When the amplitude of the back EMF is very low, the voltage drop on these devices will affect the accuracy of the zero crossing detection.

Let's do the circuit analysis again considering the voltage drop across the diode and the switch. For low voltage application, the power switch is low on-resistance MOSFET and the diode is the body diode of the MOSFET.

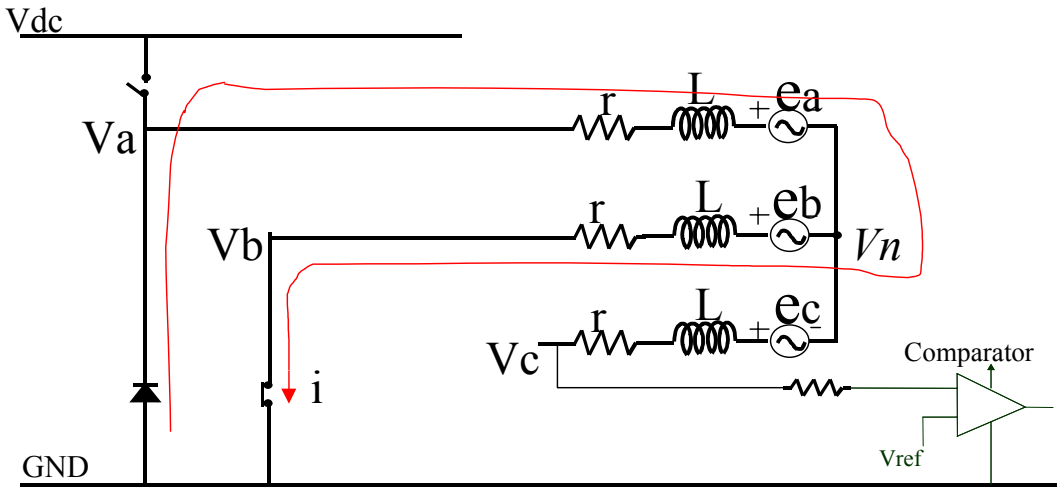

Fig.3.2 Back EMF detection circuit

Same as in chapter II, the terminal voltage of the floating phase C is calculated during PWM off period.

From phase A, we have

$$v_n = 0 - v_d - ri - L\frac{di}{dt} - e_a \quad (3.7).$$

From phase B, we have

$$v_n = v_{mos} + ri + L\frac{di}{dt} - e_b \quad (3.8).$$

Where Vd is the forward voltage drop of the diode, Vmos is the voltage drop on MOSFET.

Adding (3.7) and (3.8), we get

$$2v_n = v_{mos} - v_d - (e_a + e_b) \quad (3.9),$$

and

$$v_n = \frac{v_{mos} - v_d}{2} - \frac{e_a + e_b}{2} \quad (3.10).$$

Also from the balanced three-phase system, we have

$$e_a + e_b + e_c = 0 \quad (3.11).$$

From (3.9) and (3.10),

$$v_n = \frac{v_{mos} - v_d}{2} + \frac{e_c}{2} \quad (3.12).$$

So, the terminal voltage Vc,

$$v_c = e_c + v_n = \frac{3}{2}e_c + \frac{v_{mos} - v_d}{2} \quad (3.13).$$

If we ignore the second term of (3.13), the result is same as (2.6) in chapter II. However, at low speed and low voltage, the Back EMF itself is very small, the second

term will play a significant role here. For low voltage MOSFET, Rdson is very low, Vmos can be ignored, so (3.11) can be rewritten as,

$$v_c = e_c + v_n = \frac{3}{2} e_c - \frac{v_d}{2} \qquad (3.12).$$

Therefore, the voltage drop on the diode will bias the terminal voltage. When the back EMF e_c is high enough at high speed, the impact of the second term of (3.12) is minimum, and can be neglect. At low speed, we need to consider the effect.

To verify the analysis, we use Mathcad to simulate the circuit considering voltage drop on diodes when the amplitude of the back EMF is low.

Fig.3.4 and Fig.3.3 show the simulation and the test results respectively. Fig3.3 shows that when sine waves are biased by a offset voltage, the zero crossings are shifted, unevenly distributed. The simulation and test results validate the analysis.

Meanwhile, at low speed, the slope of the back EMF near the zero crossing is very flat. The offset and the hysteresis loop of the comparator can shift the exact zero crossing point as well.

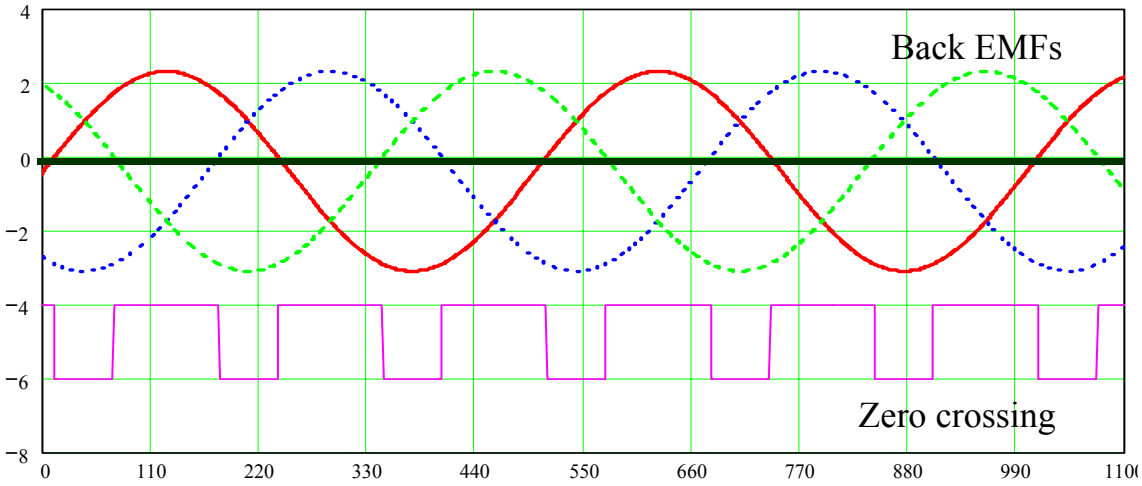

Fig.3. 3 Simulation results of back EMF zero crossing at low speed.

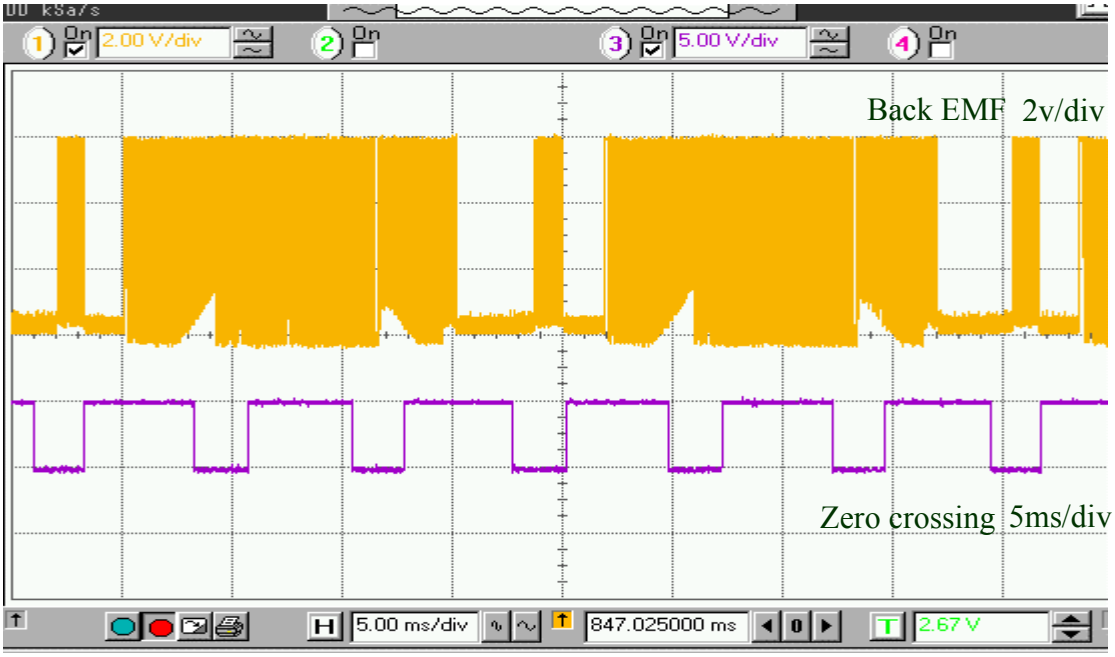

Fig.3.4 Test results of back EMF zero crossing at low speed.

3.2.2. Improved Back EMF Detection Circuit for Low speed Applications

3.2.2.1 Complementary PWM

The first method to correct the offset voltage of the back EMF signal is to use complementary PWM. In previous chapter, the PWM is applied to high side only, shown in Fig2.5. When PWM is off, the current will freewheel through the body diode of bottom switch. The voltage drop across the diode causes biasing back EMF signal.

If the complementary PWM is applied, the freewheeling current will flow through the MOSFET instead of the body diode. Both motor terminal windings are tied to ground by MOSFETs, therefore, the offset voltage caused by body diode is eliminated. The PWM algorithm is shown in Fig3.5.

Another benefit of this complementary PWM, also referred to synchronous rectification, reduces the conduction loss during the current freewheeling period.

To implement the complementary PWM algorithm, dead time is necessary to prevent cross conduction between high side and low side MOSFET in the bridge. For ST72141, it has to implement this by external components. The new version ST7MC [25] will have built-in dead time generation.

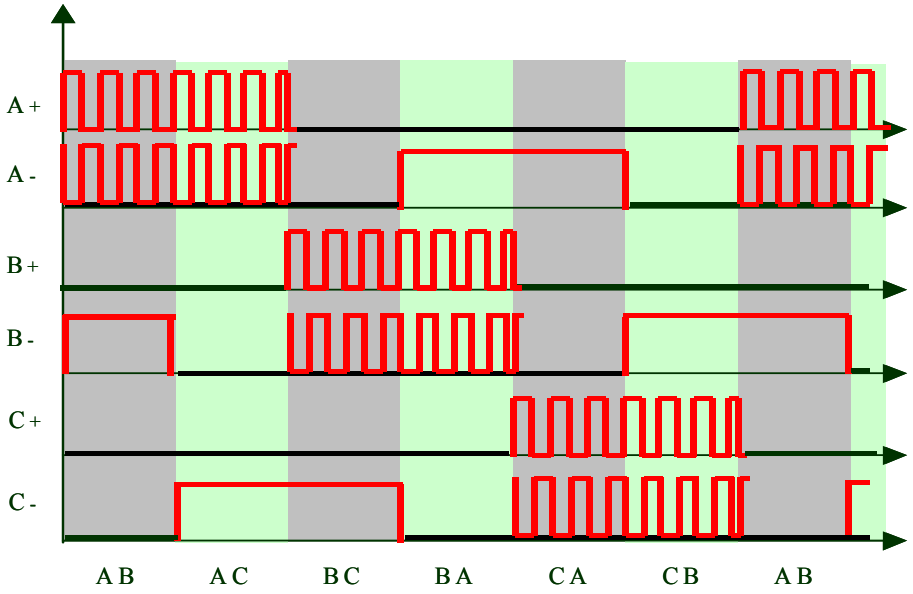

Fig.3. 5 Complementary PWM signal

Fig3.6 shows that zero crossing signal is much more balanced.

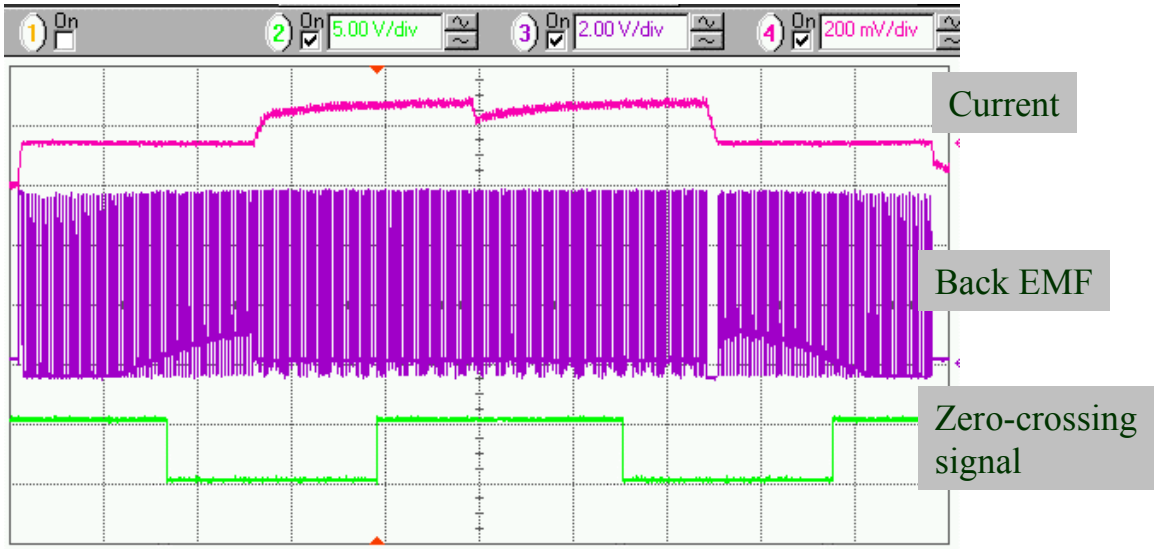

Fig.3. 6 Test result of complementary PWM

3.2.2.2 Pre-conditioning Circuit to Correct the Biased Back EMF Signal

To eliminate the effect of diode voltage drop, we can also add a compensating t voltage to compensate the effect of the diode before the back EMF signal is sent to the comparator [15].

To alleviate problem caused by offset and hysterisis voltage of the comparator, we need to sharpen the slope of the Back EMF during the zero crossing period. We can use an amplifier to amplify the Back EMF signal.

A pre-conditioning circuit for back EMF zero crossing detection is developed to compensate the diode voltage drop and sharpen the slope of the back EMF signal near the zero crossing. The pre-conditioning circuit is shown in Fig.3.7.

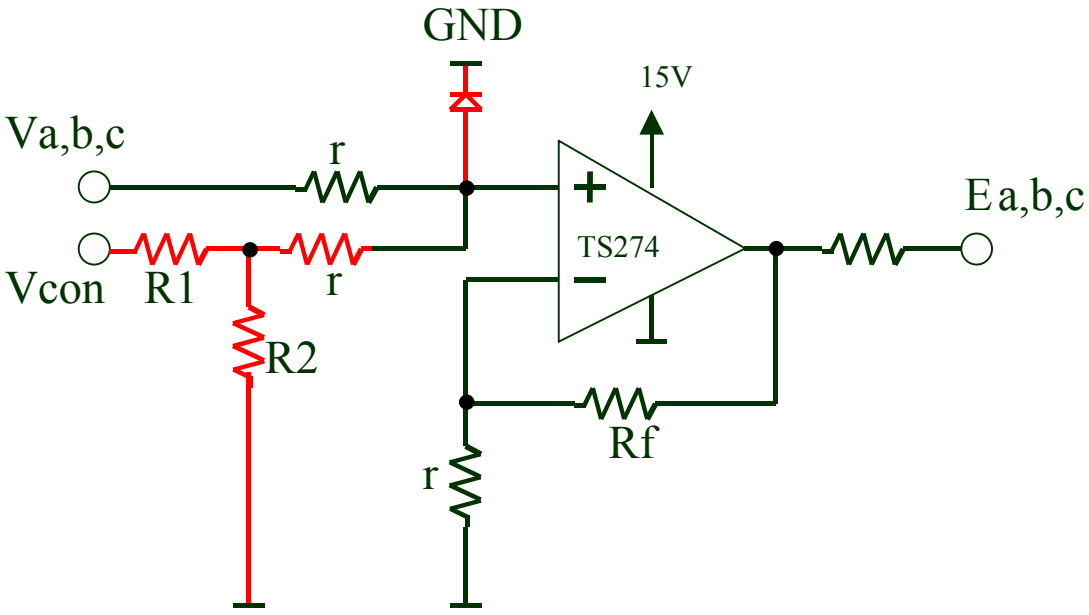

Fig.3. 7 A pre-conditioning circuit for back EMF zero crossing detection.

TS274 is a high speed Op-amp. Chose R1 and R2 such that Vcon*R2/(R1+R2)=V_d/2. The positive input of the Op-amp is clamp at 0.7v by a diode because only signal close to zero crossing is of interest. So we only sharpen the slope of the back EMF near the zero crossing.

The positive input of the OP AM is

$$V_+ = V_x + V_{con} * \frac{R_2}{R_1 + R_2} \tag{3.13}$$

where Vx can be Va, Vb or Vc, terminal voltage of three windings.

From previous analysis,

$$v_x = \frac{3}{2} e_x - \frac{v_d}{2} \tag{3.14}.$$

If let $V_{con} * \frac{R_2}{R_1 + R_2} = \frac{V_d}{2}$, then

$$V_+ = \frac{3}{2} e_x \tag{3.15}$$

The output of the OP AM will be

$$E_x = (1 + Rf / r) * \frac{3}{2} e_x \tag{3.16}$$

Therefore, this pre-conditioning circuit not only eliminates the offset caused by voltage on diode, but also sharpens the slope of the back EMF signal by amplifying the signal.

Fig.3.8 and Fig.3.9 show the result of the pre-conditioning circuit.

In Fig.3.8, the amplitude of the back EMF is very low. If there is no pre-conditioning circuit, the zero crossing point is A. the pre-conditioning circuit not only compensates the offset, but also sharpens the slope of the signal near the zero crossing. The zero crossing point is detected at B with the pre-conditioning circuit. Pay attention that amplitude voltage scaling for two signals is 10 times difference.

Fig.3.8 The upper channel: input signal to the pre-conditioning circuit; middle channel: output signal from the pre-conditioning circuit; lower channel: zero crossing detected.

Fig.3.9 shows that zero crossings are evenly distributed after the pre-conditioning circuit is used.

Fig.3.9 Improved zero crossing detection by pre-conditioning circuit.

This improved circuit further extends the application of the sensorless BLDC drives. For conventional back EMF detection scheme, the speed range of the motor (maximum speed verse minimum speed) is typically about 5:1. For the proposed back EMF detection scheme without the pre-conditioning circuit, the speed range can be up to 10:1. The speed range can be extended to at least 50:1, if the pre-conditioning circuit is used. Fig3.10 shows the three-phase pre-conditioning circuit.

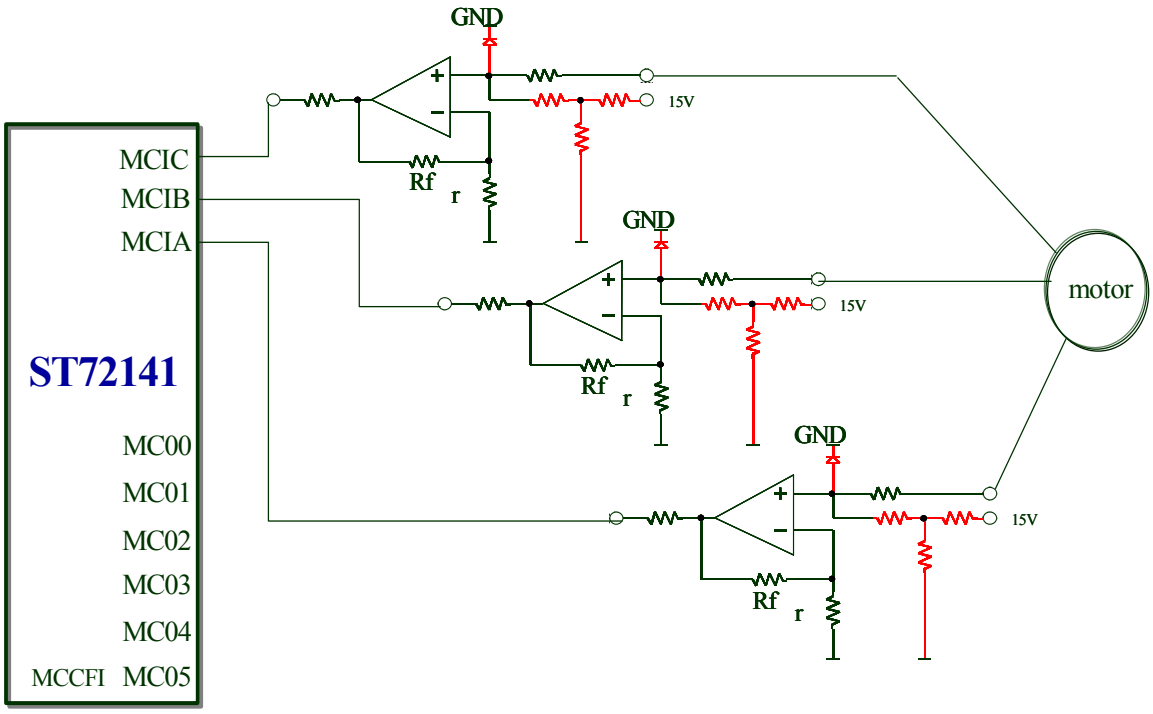

Fig.3. 10 Three phase pre-conditioning circuit

3.3 Improved Circuit for High Voltage Applications

In chapter II, it is mentioned that three phase terminal voltages are directly fed into the microcontroller through resistors, which limit the injected current. For different voltage applications, we need to choose different resistance accordingly. The injected current should be limited around 2 mA. For some household appliance applications, the dc bus voltage can be 300 v. The resistor value is chosen 160kΩ.

We find that zero crossing detection is not correct sometime when PWM duty cycle is high. The problem is caused by the large time constant of the current limit resistors. Inside the microcontroller, there is some parasitic capacitance. Since the outside resistance is high enough, even though the capacitance is low, the effect of RC time constant will show up. Fig.3.7 shows the winding terminal voltage Vmc and the voltage V_C at the input pin of the microcontroller.

It is clear that V_C has different delay time at the rising edge and the falling edge. The falling edge can last about 10us and the rising edge is very fast. The reason that causes the different slope is different exciting voltage source for the RC circuit. At the rising edge, the exciting source is motor terminal voltage. Since the terminal voltage is high (~300 v), the injecting current can charge the capacitor quickly. So the rising edge is short. At the falling edge, discharging source voltage is only 5v, thus, the discharging current is very small. Therefore, the falling edge is far longer than rising edge.

The back EMF signal is sampled at the end of PWM off time. If the PWM duty cycle is high enough such that the off time is less than 10us, the sampling result is not correct because the discharging period hasn't finished yet.

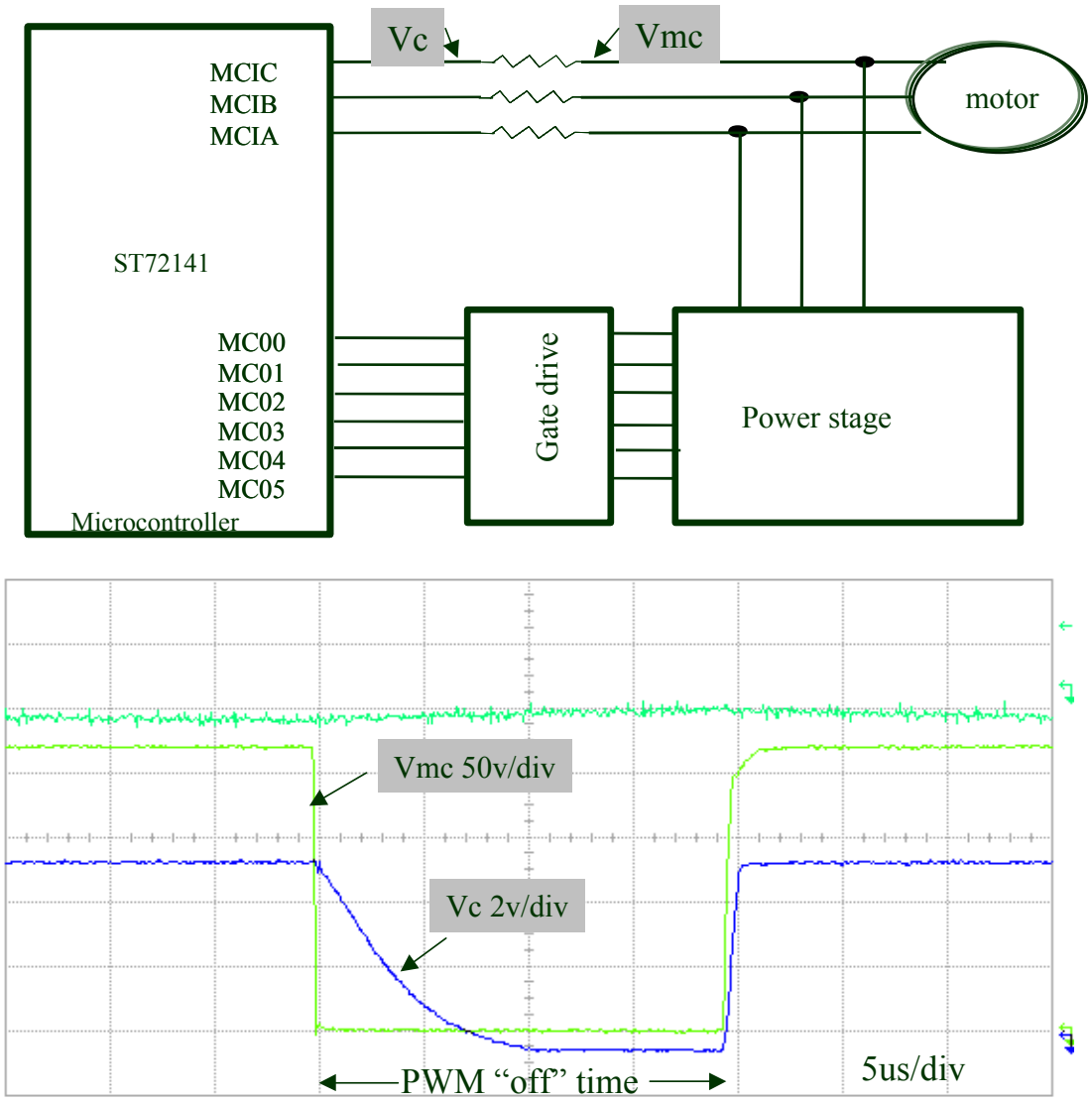

Fig.3.11 Waveform of winding terminal voltage and voltage at the input pin of the Micro

Fig.3.12 shows the equivalent circuit for charging and discharging of the parasitic capacitor.

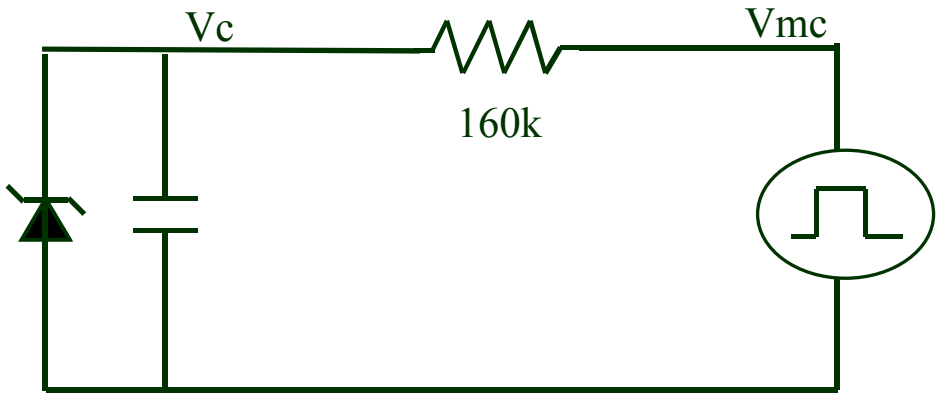

Fig.3.12 Equivalent circuit for charging and discharging of the parasitic capacitor.

To shorten the discharging time, we should reduce RC time constant. We can't change the capacitance, but we can change the resistor value. Fig.3.13 shows a circuit that different time constants for rising edge and falling edge. At the rising edge of Vmc, Vmc will charge the capacitor through the 160k resistor. At the falling edge of Vmc, the discharging period, and the diode will forward conduct and the capacitor will be discharged through 20k resistor. Fig.3.14 shows the test result of circuit with variable RC time constant. The discharging time is about only 1us.

Fig.3.15 shows the schematic of the improved circuit of back EMF detection for high voltage applications.

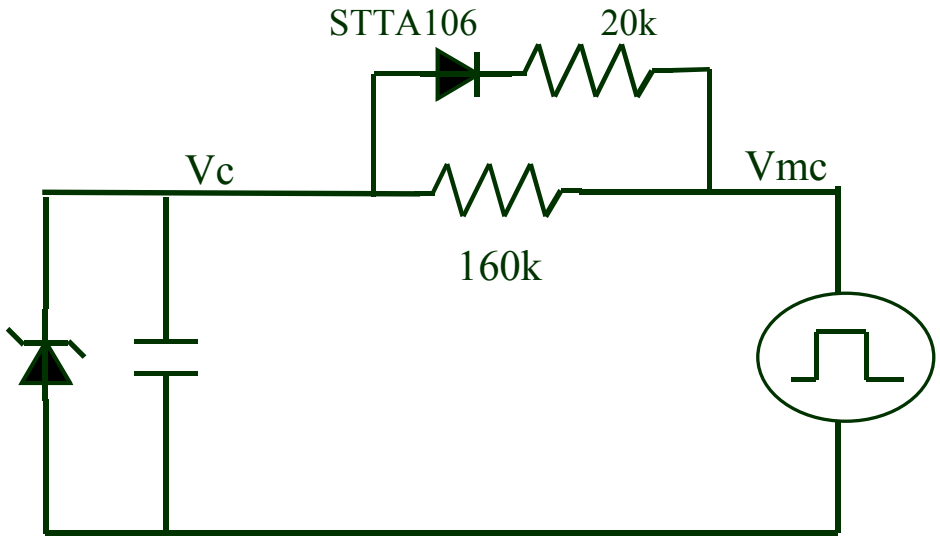

Fig.3.13 Circuit of different time constants for charging and discharging.

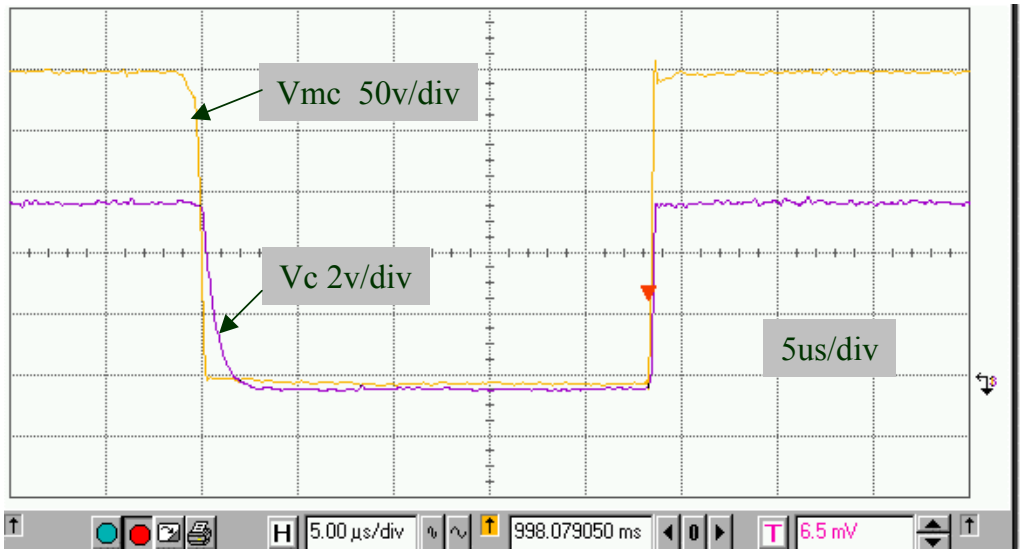

Fig.3. 14 Test result of variable RC time constant circuit.

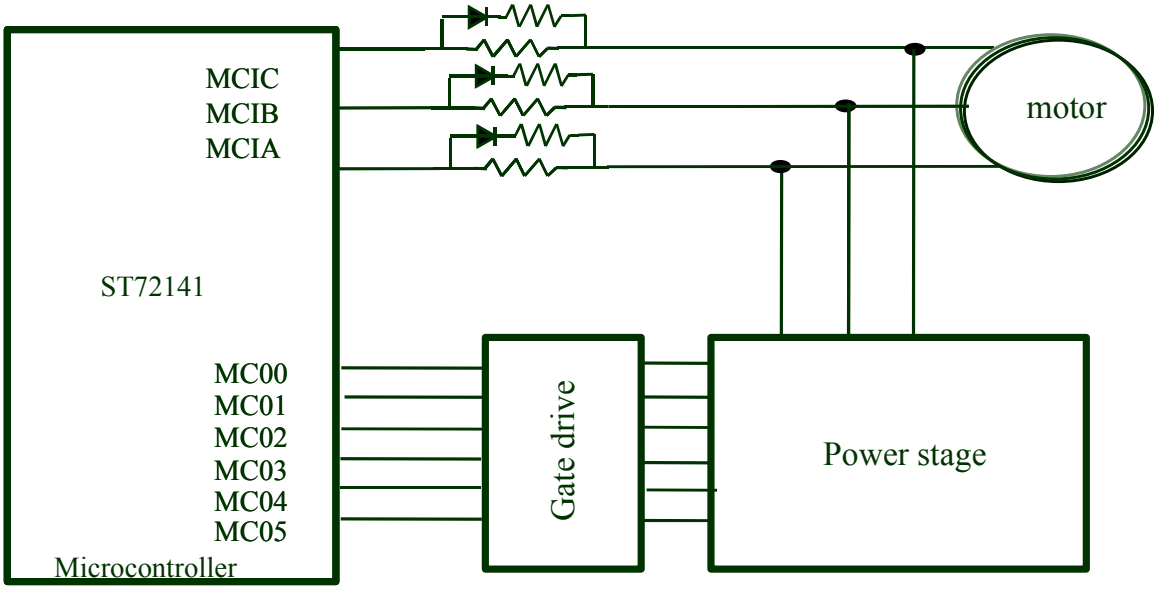

Fig.3.15 Improved back EMF detection circuit for high voltage applications.

3.4. Summary

In this chapter, improved circuitry for low speed /low voltage and high voltage applications are described.

The limitation of the back EMF detection during off time is that there is a requirement to have a minimum off time. Sometime this is undesirable for low voltage applications. An alternate back EMF detection during on time is proposed to make the duty cycle up to 100%, thus the bus voltage can be fully utilized.

The complementary PWM algorithm is proposed to eliminate the offset voltage caused by the body diode voltage when current is freewheeling through the diode. The offset voltage can cause untruthful zero crossing detection, especially at low speed.

The pre-conditioning circuit for low speed applications not only compensates the offset voltage caused by diodes, but also sharpens the slope of the back EMF signal near the zero crossing.

The variable time constant of the back EMF sensing circuit avoids the long falling edge of signals caused by large RC time constant.

The improved circuitry greatly expands the motor speed range. For example, for a 48 V motor, the speed operation range can be from 50rpm to 2500rpm. For high voltage operation, the sensorless system has been successfully used for 300v/30,000 rpm high-speed air blower applications.

Chapter IV

Starting the Motor with the Sensorless Scheme

4.1 Introduction

The sensorless schemes are not self-starting. In order to sense the back EMF, the motor must be first started and brought up to a certain speed where the back EMF voltage can be detected. In practice, open-loop [16] starting the motor is accomplished by providing a rotating stator field with a certain increasing frequency profile. Once the rotor field begins to become attracted to the stator field enough to overcome friction and inertia, the rotor will turn. After the speed reaches a threshold voltage value, the back EMF can be detected, providing the position information, the system switches to synchronous commutation mode and the motor acts as a permanent magnet synchronous machine. If there is no specific requirement for start-up, like fans application, this open loop start-up can be satisfactory. However, for some applications, i.e., automotive fuel pump, the start-up has to be finished with 200ms to build up the pressure. It is very difficult to tune the start-up using the open-loop starting algorithm. On the other hand, if the starting torque is medium or high, usually it is difficult to start the motor with the open-loop algorithm.

In this section, a practical start-up tuning procedure with the help of a dc tachometer will be descried. The commutation during start-up is tuned in this way such that the

motor speed has the maximum acceleration. This procedure is generally applicable for all different sensorless BLDC systems.

4.2 Test set-up

Connect motor with the load/dyno and a dc tachometer along the shaft through joint couplers. The output of the tachometer is a dc voltage that is directly proportional to the speed. From the tachometer voltage, we will know the instant speed of the motor. Fig. 4.1 shows the set-up.

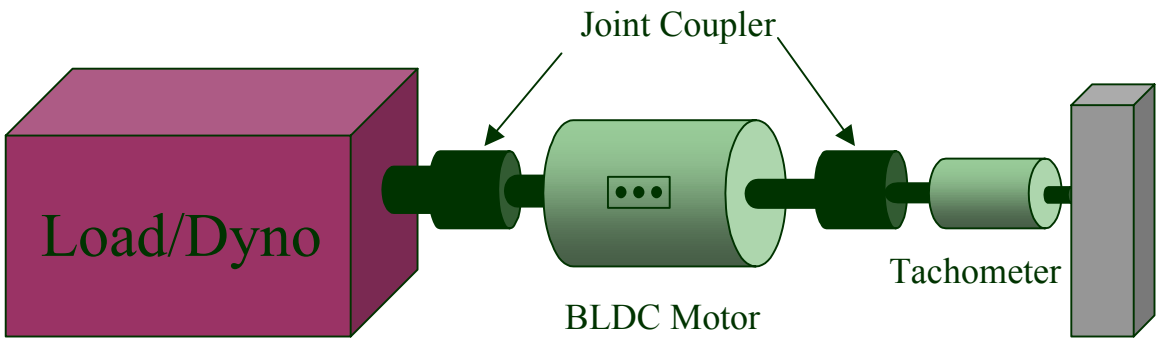

Fig.4.1 Test set-up for tuning motor starting.

4.3 Start-up Tuning Procedure

When the motor stops, the controller doesn't know the rotor initial position. The first step is to align the motor to a known position by exciting two phases of the motor. For instance, we can choose phase A and phase B to be excited to set the initial position. After the rotor is in the initial position, a preset exciting pattern will be sent out. If three phases are alternately excited, the motor will start to accelerate. Table 4.1 and 4.2 show the exciting pattern for forward /backward rotation. The motor is driven with 6-step mode, and the exciting phase just repeats the same pattern after one cycle (6 steps).

Table 4.1 Phase exciting pattern for forward rotation

	Alignment (Step 0)	Step 1	Step 2	Step 3	Step 4	Step 5
Exciting phases	AB	AC	BC	BA	CA	CB

Table 4.2 Phase exciting pattern for backward rotation

	Alignment (Step 0)	Step 1	Step 2	Step 3	Step 4	Step 5
Exciting phases	AB	CB	CA	BA	BC	AC

The question is how to set the right time for each step. If we know the instant motor speed, we set the time for each step so that the motor speed keeps accelerating. We can get the instant motor speed from the dc tachometer.

We take forward rotation as an example for the start-up tuning.

Before starting, the position of the rotor is unknown. A pre-positioning is needed to place the motor in a known position. The pre-positioning is also called alignment. After phase A and phase B is excited, the rotor will align with the flux direction generated by phase A and phase B.

When the rotor approaching the alignment position, it will oscillate. The output of the tachometer will tell how long the oscillation lasts. Fig.4.2 shows current of phase A and the oscillation waveforms during the pre-positioning period. In order to reduce the oscillation, a progressive ramp-up current can be set to bring the rotor into the desired position. Applying a strong current level directly to the windings will make the rotor move more quickly and in turn this will make it oscillate more severe around the final position.

The pre-positioning period has to be long enough that the oscillation stops. Otherwise, the rotor will be at unknown position if it is still oscillating. In Fig.4.2, the time period, from T0 to T1, is the pre-positioning period. The oscillation stops before the end of pre-positioning. The tachometer signal shows the oscillation of the rotor.

After the pre-positioning phase is finished, the motor can be commutated to first step, phase A and C conducting current. At beginning of this commutation, the motor will start to turn because accelerating torque is produced. However, If this step lasts too long, the motor speed will first increase and then decrease. Fig.4.3 shows the waveform.

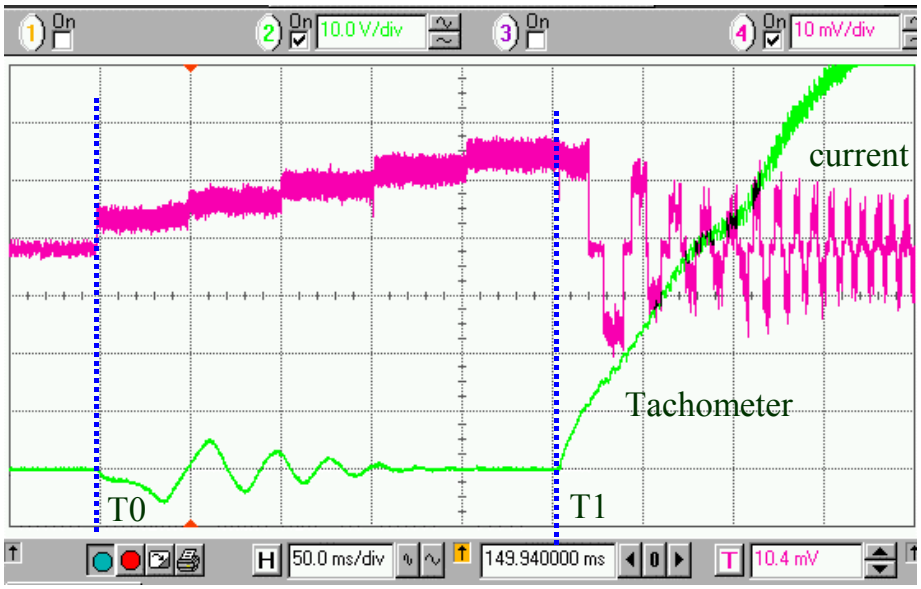

Fig.4.2 Pre-positioning before starting the motor.

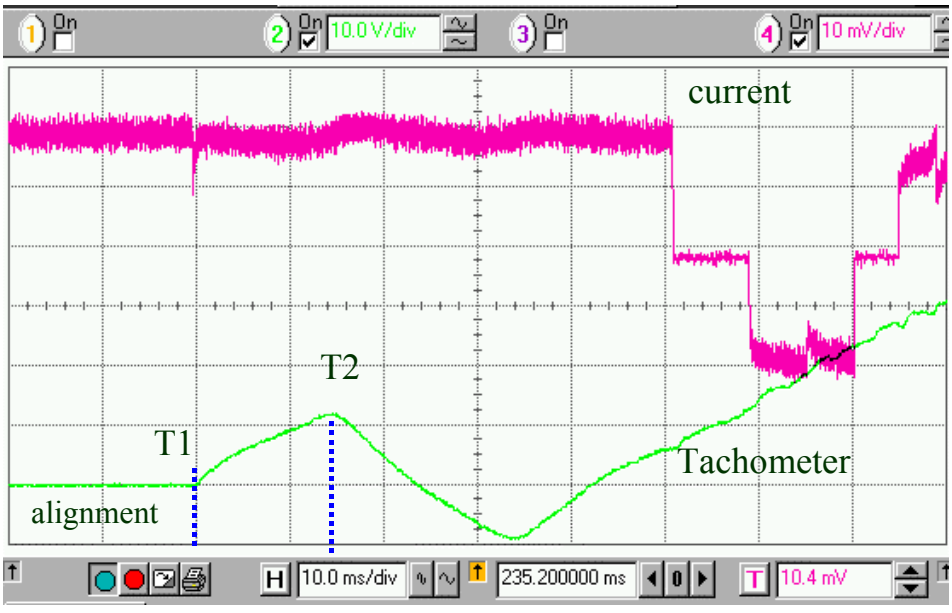

Fig.4.3 Current and tachometer waveform at the first step.

From the waveform, the speed of the motor rises from time T1, until time T2, since this step is set too long. So we should set time for this step as T2-T1. At time T2, the motor should commutate forward to next step.

The second step is when phase B and phase C are excited according to Table 4.1. Similarly, we set the step time very long first and watch the output of the tachometer. From Fig.4.4, we can find the right time, T3-T2, for the second step.

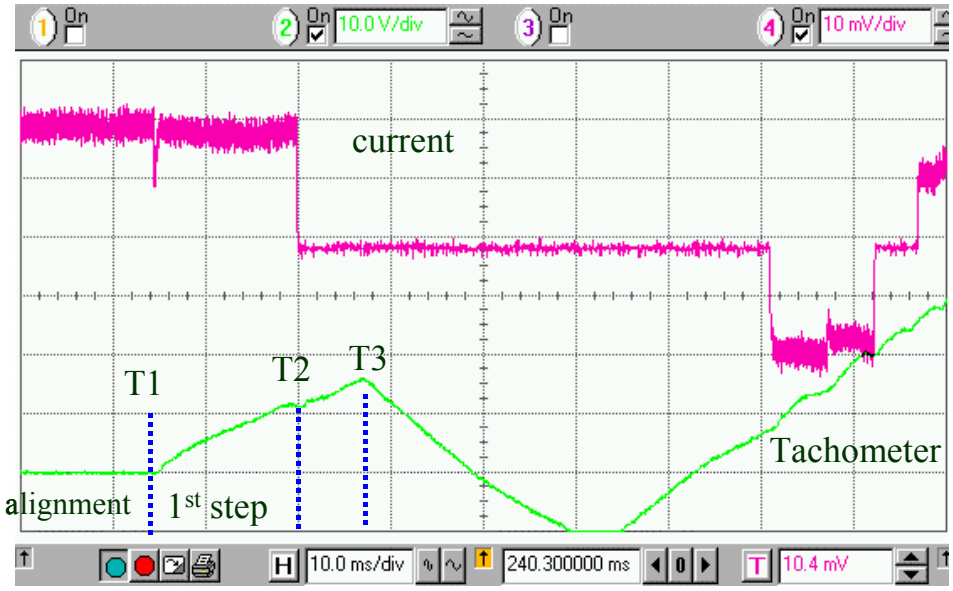

Fig.4.4 Current and tachometer waveform at the second step.

Continue to do the tuning, we can get the right time for following steps until the microcontroller can detects the back EMF and switches to synchronous commutation mode. With the help of the tachometer, we can have the best acceleration during the start-up.

Fig.4.5 shows the final result of the starting.

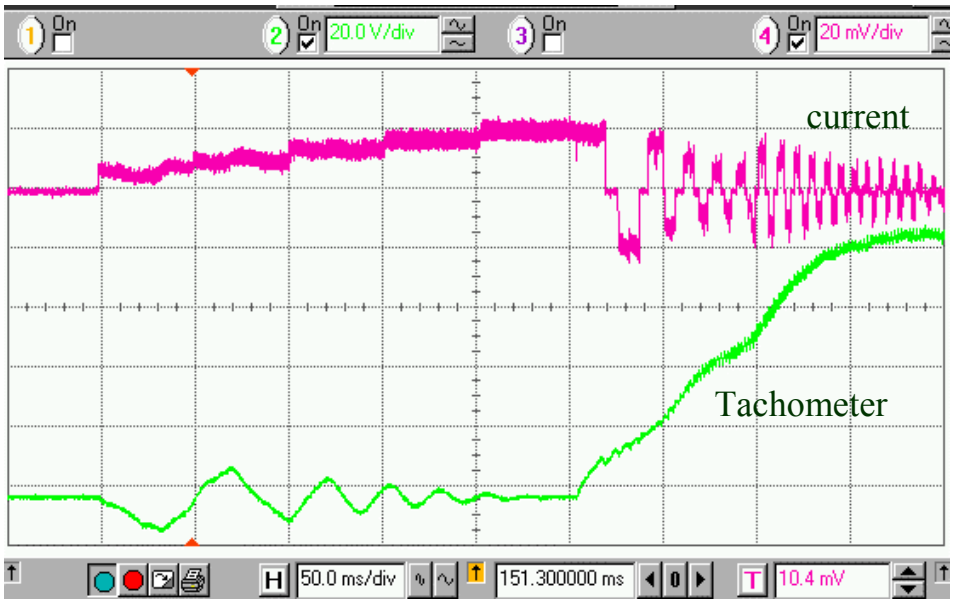

Fig.4.5 Current and Tachometer waveform during start-up period.

Chapter V

Conclusions and Future Research

5.1 Conclusions

The applications of brushless DC (BLDC) motors and drives have grown significantly in recent years in the appliance industry and the automotive industry. Sensorless BLDC drive are very preferable for compact, low cost, low maintenance, and high reliability system. The conventional sensorless method based on neutral motor point has limited its application since it has relative speed range, suffering from high common mode voltage noise and high frequency switching noise. In this thesis, a novel back EMF sensing technique, direct back EMF sensing, without motor neutral voltage for BLDC drives is proposed, analyzed, and extended, overcoming the drawbacks of the conventional scheme.

The direct back EMF sensing scheme avoids the motor neutral point as the reference for the back EMF zero crossing detection. In this scheme, the PWM is applied to high side switches of the inverter, the back EMF is measured during the PWM off time in the floating winding. It is proved that the terminal voltage of the floating winding is directly proportional to the back EMF of that phase.

Several advantages of the direct back EMF sensing scheme are summarized in the following.

i. The scheme can detect the back EMF with very high resolution, because it doesn't have signal attenuation;

ii. The switching noise is rejected by synchronous sampling;

iii. There is no filtering to cause phase shift or delay;

iv. There is no common mode voltage noise issue.

A synchronous sampling circuit for the back EMF sensing is developed, and the circuit is integrated with a standard low cost 8-bit microcontroller to be a dedicated BLDC sensorless drive controller. This microcontroller has been commercialized and applied in real applications such as automotive fuel pumps and home appliances.

An improved version of the direct back EMF sensing, detecting the back EMF signal during PWM on time, is presented. Since the original method detects back EMF signal during PWM off time, it can't go to 100% duty cycle. The improved method will overcome the duty cycle limit.

The complementary PWM algorithm can eliminate the offset voltage in the back EMF signal caused by the voltage drop of the diode, and also increase the system efficiency by reducing the conduction loss. The pre-conditioning circuit not only compensates the offset voltage, but also amplifies the back EMF signal to be stronger. This extends the sensorless BLDC motor drive system to much wider speed range.

A variable time constant sensing circuit for high voltage application is presented to solve the unexpected delay issue caused by parasitic capacitance in the circuit.

Sensorless BLDC system is not self-starting system. The traditional frequency profile ramping method can't fit for all different applications. In the thesis, a start-up procedure with help of a tachometer is established. The start-up tuning procedure has optimized start-up performance and it is suitable for all sensorless BLDC motor drive systems.

5.2 Future Research

The start-up tuning described in chapter IV is done by manually. Future work is desired to achieve an automated maximum acceleration start-up. Machine saliency could be used for rotor position estimation [21].

New machine design also is an alternate solution to sensorless operation. Some research is going on to add the special sensing winding to the machine to indicate the rotor position [22]. There are no Hall-type sensors, therefore, the system is robust.

The design of BLDC motor is not standardized yet. Optimized design of the BLDC motor that achieves higher efficiency with lower cost is desirable.

Reference

[1] Thomas Kaporch, “Driving the future,“ Appliance Manufacture, Sept.2001, pp43-46.

[2] Joe Mattingly, “More Efficiency Standards on Horizon,” Appliance Manufacture, Oct.2001, Published on Internet.

[3] J.Filla, “ECMs Move into HVAC,” Appliance Manufacture, Mar.2002, pp25-27.

[4] J.Jancsurak, “Motoring into DSPs,” Appliance Manufacture, Sept.2000, pp57-60.

[5] T.J.E. Miller, “ Brushless Permanent-Magnet and Reluctant Motor Drives,” Oxford, 1989.

[6] K.Rajashekara, A.Kawamura, et al, “Sensorless Control of AC Motor Drivers,” IEEE press, 1996.

[7] US Patent No.4654566, “ Control system, method of operating an electronically commutated motor, and laundering apparatus,” granted to GE.

[8] K.Uzuka, H.Uzuhashi, et al., “Microcomputer Control for Sensorless Brushless Motor ,” IEEE Trans. Industry Application ,vol.IA-21, May-June, 1985.

[9]. R.Becerra, T.Jahns, and M.Ehsani, “Four Quadrant Sensorless Brushless ECM Drive,” IEEE Applied Power Electronics Conference and Exposition 1991, pp.202-209.

[10]. J.Moreira, “Indirect Sensing for Rotor Flux Position of Permanent Magnet AC Motors Operating in a Wide Speed Range,” IEEE Industry Application Society Annual Meeting 1994, pp401-407.

[11]. S.Ogasawara and H.Akagi, “ An Approach tp Position Sensorless Drive for Brushless dc Motors,” IEEE Trans. on Industry Applications, Vol.27, No.5, Sept/Oct. 1991.

[12] D.Peter and J.Hath, “ ICs Provide Control for Sensorless DC Motors,” EDN magazine, pp.85-94, April 1993.

[13]. Datasheet of ML4425 from Fairchild Semiconductor.

[14]. Datasheet of A8902CLBA from Allegro Micro Systems.

[15] J.Shao, D.Nolan, and T.Hopkins, “A Novel Direct Back EMF Detection for Sensorless Brushless DC (BLDC) Motor Drives,” Applied Power Electronic Conference (APEC 2002), pp33-38.

[16] J.Johnson, “Review of Sensorless Methods for Brushless DC,” IAS, pp143-150, 1999.

[17] ST72141 datasheet from STMicroelectronics

[18] US Patent 5859520, “Control of a Brushless Motor,” granted to STMicroelectronics.

[19] US Patent Application, “Circuit for Improved Back EMF Detection,” STMicroelectronics.

[20] R.Krishnan and R. Ghosh, “Starting Algorithm and Performance of a PM DC Brushless Motor Drive System with No Position Sensor,” IEEE PSEC 1989, pp.815-821.

[21] N.Mastui, " Sensorless PM Brushless DC Motor Drives," IEEE Trans. on Industrial Electronics, Vol. 43, April 1996.

[22] D.E.Hesmondhalgh, D. Tipping, and M.Amrani, " Performance and Design of an Electromagnetic Sensor for Brushless DC Motors," IEE Proc. Vol.137, May 1990.

[23] J.Shao, D.Nolan, T.Hopkins, " A Novel Microcontroller-based Sensorless Brushless DC (BLDC) Motor Drive for Automotive Fuel Pumps," Industry Applications Annual Meeting IAS'2002.

[24] J.Shao, D.Nolan, T.Hopkins, "A Direct Back EMF Detection for Sensorless Brushless DC (BLDC) Motor Drive and the Start-up Tuning," Power Electronics Technology Conference (Formerly PCIM) 2002.

[25] Preliminary datasheet of ST7MC from STMicroelectronics.

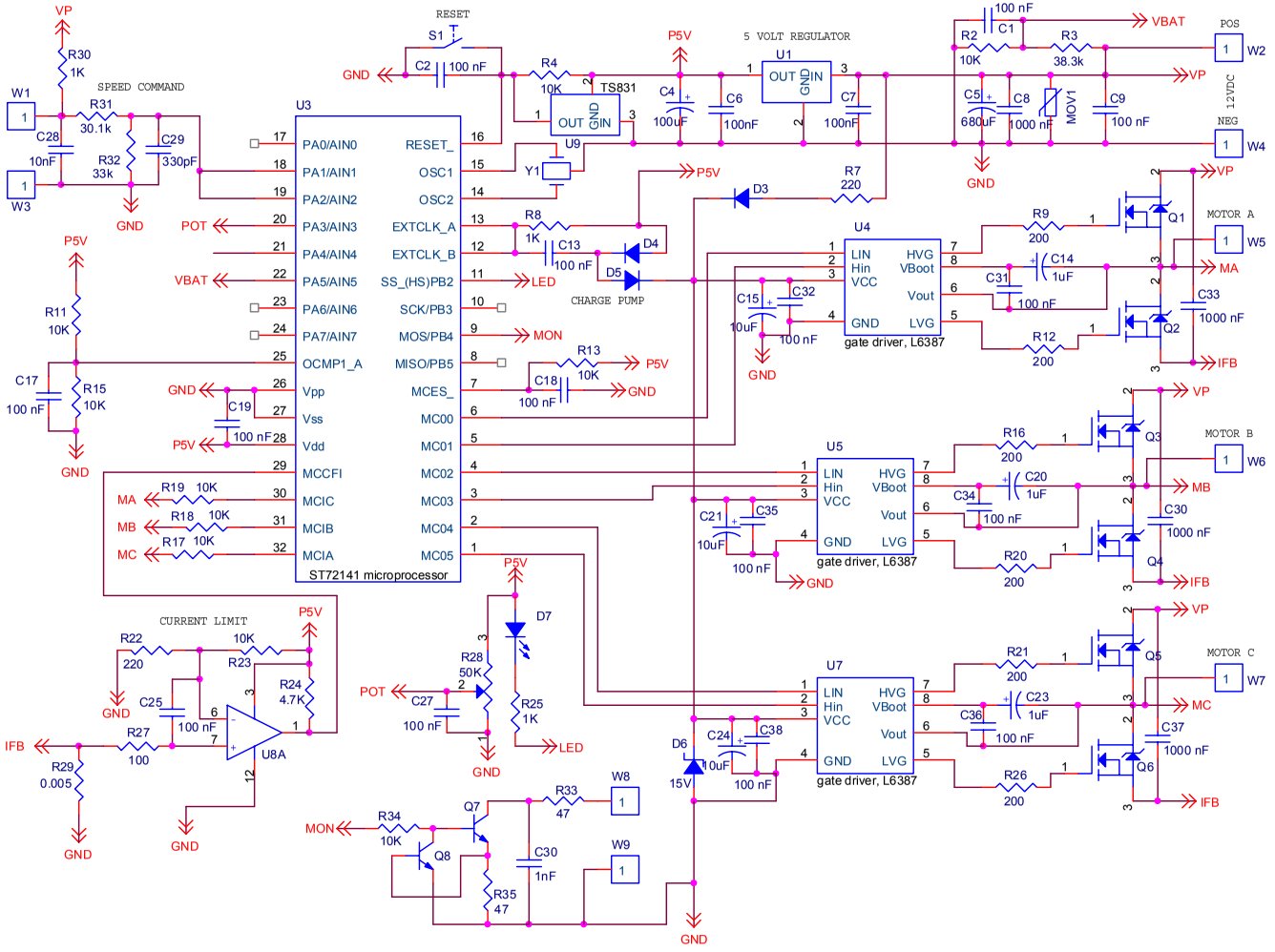

Apendix1 schematic of sensorless BLDC motor drive for low voltage applications.

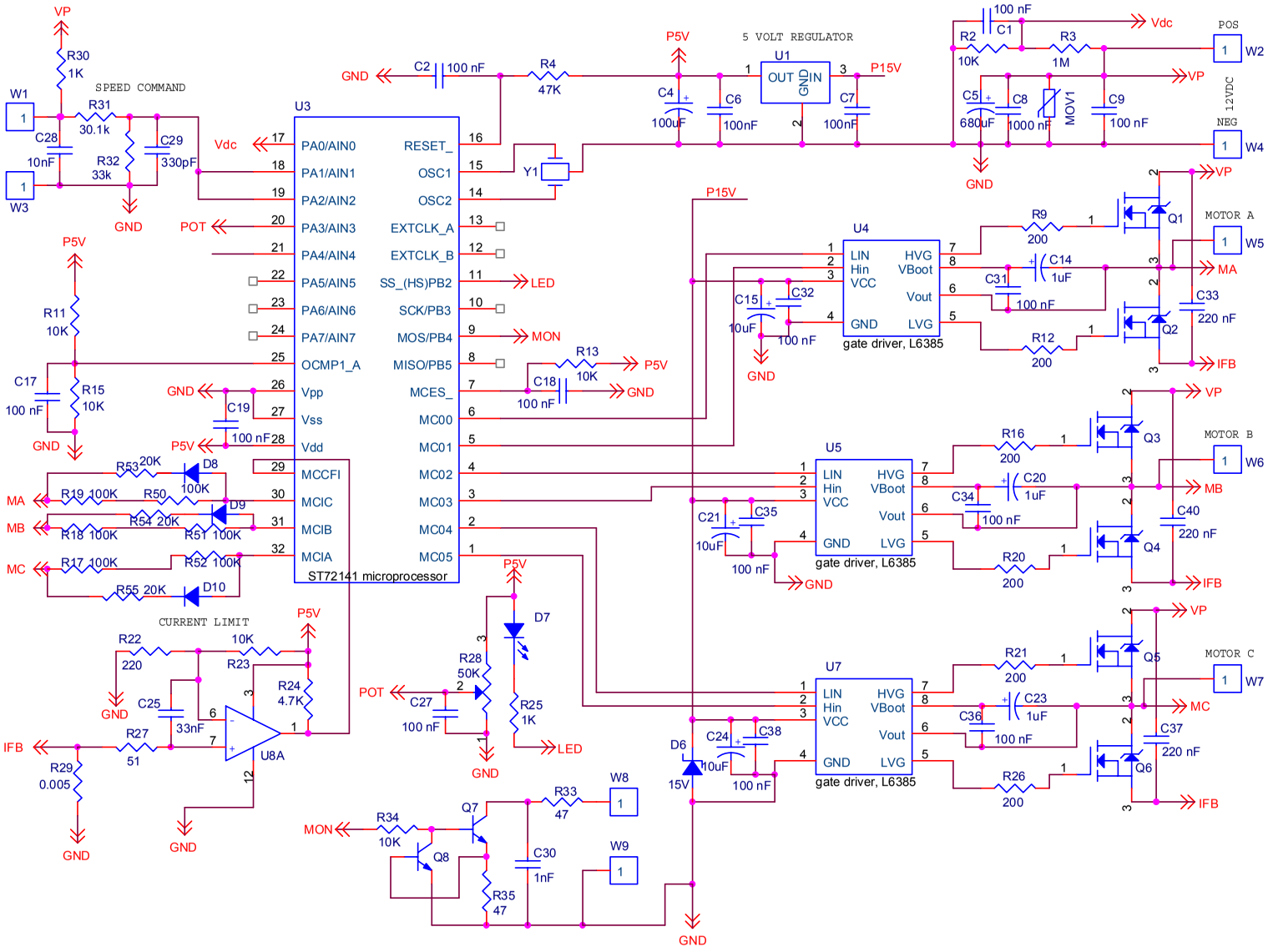
VP
R30
1K
SPEED COMMAND
W1
R31
30.1k
C28
10nF
R32
33k
C29
330pF
W3
GND
Vdc
POT
U3
PA0/AIN0
PA1/AIN1
PA2/AIN2
PA3/AIN3
PA4/AIN4
PA5/AIN5
PA6/AIN6
PA7/AIN7
OCMP1_A
Vpp
Vss
Vdd
MCCFI
MCIC
MCIB
MCIA
RESET_
OSC1
OSC2
EXTCLK_A
EXTCLK_B
SS_(HS)PB2
SCK/PB3
MOS/PB4
MISO/PB5
MCES_
MC00
MC01
MC02
MC03
MC04
MC05
ST72141 microprocessor
LED
MON
P5V
R11
10K
C17
100 nF
R15
10K
C19
100 nF
R53 20K
D8
R19 100K
R50
100K
D9
MA
R54 20K
MB
R18 100K
R51 100K
R17 100K
MC
R52 100K
R55 20K
D10
CURRENT LIMIT
R22
220
R23
10K
R24
4.7K
C25
33nF
R27
51
IFB
R29
0.005
U8A
C2
100 nF
R4
47K
Y1
5 VOLT REGULATOR
U1
OUT
GND
IN
P15V
C4
100uF
C6
100nF
C7
100nF
C1
100 nF
R2
10K
R3
1M
C5
680uF
C8
1000 nF
MOV1
C9
100 nF
POS
W2
12VDC
NEG
W4
C18
100 nF
R13
10K
U4
LIN
Hin
VCC
HVG
VBoot
Vout
LVG
gate driver, L6385
C15
10uF
C32
100 nF
C14
1uF
C31
100 nF
R9
200
R12
200
Q1
Q2
MOTOR A
W5
C33
220 nF
U5
C21
10uF
C35
100 nF
C20
1uF
C34
100 nF
R16
200
R20
200
Q3
Q4
MOTOR B
W6
C40
220 nF
U7
C24
10uF
C38
100 nF
C23
1uF
C36
100 nF
R21
200
R26
200
Q5
Q6
MOTOR C
W7
C37
220 nF
D7
R28
50K
C27
100 nF
R25
1K
D6
15V
R33
47
W8
W9
R34
10K
Q7
Q8
C30
1nF
R35
47

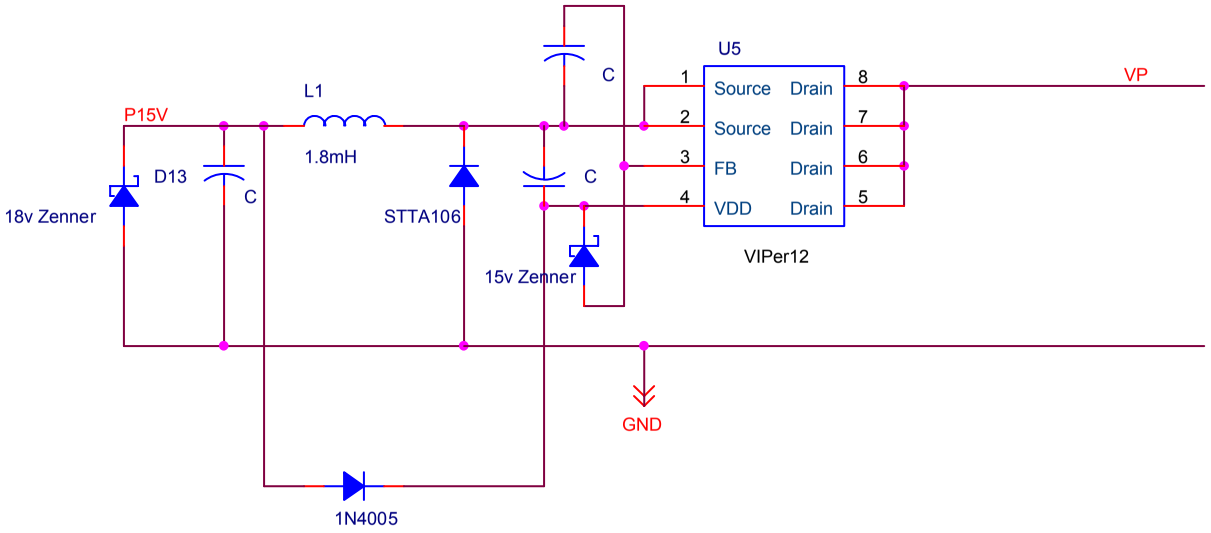

Apendix2 schematic of sensorless BLDC motor drive for high voltage applications.

VITA

Jianwen Shao

The author received his Bachelor of Engineering and Master of Engineering degree from Tsinghua University, China, in 1992 and 1995. From 1995 to 1998, he worked as lead electrical design engineer in Beijing CATCH New Technology Inc. to develop the high power, low harmonic multilevel inverters for industrial applications. He finished his Master courses study in Virginia Tech from 1998 to 2000. He has been conducting research in the area of motor drive, power factor correction, and high frequency inverters.